



# ICEYE X4, X6 and X7 Quality Assessment Summary

Author(s):



**Jorge Jorge Ruiz, Juval Cohen**

*Task 3 Mission Expert*

Approval:



**Davide Giudici, Aresys**

*Task 3 Lead*

Accepted:



**Clement Albinet**

*ESA Technical Officer*

## AMENDMENT RECORD SHEET

The Amendment Record Sheet below records the history and issue status of this document.

ISSUE	DATE	REASON
1.0	30/11/2021	First version
2.0	17/02/2022	Revised after comments from ESA

## ACRONYMS

AEP	Antenna Elevation Pattern
ALE	Absolute Localization Error
CEP90	Circular Error at the 90% Percentile
CR	Corner Reflector
DEM	Digital Elevation Model
FTP	File Transfer Protocol
ENL	Equivalent Number of Looks
ESA	European Space Agency
FMI	Finnish Meteorological Institute
GIS	Geographic Information System
GRD	Ground Range Detected
HDF	Hierarchical Data Format
IRF	Impulse Response Function
ISLR	Integrated Side Lobe Ratio
JPL	Jet Propulsion Laboratory
NA	Not Applicable
NESZ	Noise Equivalent Sigma Zero
NLS	National Land Survey
PSLR	Peak Side Lobe Ratio

RD	Reference Document
SL	SpotLight
SLC	Single Look Complex
SLH	SpotLight High
SM	StripMap
SNAP	SeNtinel Application Platform
SQT	SAR Quality Toolbox
STD	STandard Deviation
UTM	Universal Transverse Mercator

## TABLE OF CONTENTS

<b>AMENDMENT RECORD SHEET</b> .....	<b>2</b>
<b>1. EXECUTIVE SUMMARY</b> .....	<b>4</b>
1.1 Mission Quality Assessment Matrix .....	6
<b>2. MISSION ASSESSMENT OVERVIEW</b> .....	<b>7</b>
2.1 Product Information .....	7
2.2 Product Generation .....	9
2.3 Ancillary Information.....	9
2.4 Uncertainty Characterisation .....	10
2.5 Validation.....	11
<b>3. DETAILED ASSESSMENT</b> .....	<b>13</b>
3.1 IRF Analysis .....	17
3.1.1 X4.....	21
3.1.2 X6.....	22
3.1.3 X7.....	24
3.2 Equivalent Number of Looks (ENL).....	25
3.3 Noise Equivalent Sigma Zero (NESZ) .....	28
3.4 Elevation Antenna Pattern .....	29
3.5 Radiometric Stability .....	34
3.6 Data Processing in SNAP – Geolocation Accuracy.....	35
<b>4. CONCLUSIONS</b> .....	<b>37</b>
<b>5. REFERENCES</b> .....	<b>38</b>

## 1. EXECUTIVE SUMMARY

The ICEYE constellation is formed by several relatively small satellites, each one weighted under 100 kg. The large constellation enables different angle imaging of specified areas of interest multiple times a day, thus allowing quick tactical acquisitions as well as frequent revisit rates globally. The ICEYE SAR constellation is continuously growing and includes improvements in the individual satellites.

Quality assessment was performed on ICEYE's X4-X7 SAR satellite's Single Look Complex (SLC) products, following the EDAP assessment guidelines. The assessed data included the Stripmap (SM), Spotlight (SL) and Spotlight High resolution (SLH) imaging modes. The X4 and X5 satellites were launched in July 2019, and the X6 and X7 in September 2020. The assessment is divided into two main parts: Documentation review and an analysis of the test datasets. The document review in sections 2.1-0 includes the assessment of the documentation provided by ICEYE. The grading of these documents is given in columns 1-4 of the maturity matrix shown in section 1.1. Section 2.5 summarizes the data assessment performed by the Finnish Meteorological Institute (FMI) using the test data delivered for the EDAP project. The grading for this is given in the last column of the maturity matrix. Chapter 3 provides more detailed explanations on the methods and the results of the data analysis performed by FMI. A similar assessment has been previously performed for ICEYE's X2 satellite, which final report is available in the European Space Agency (ESA) EDAP project's web page.

The newest and the previous versions of the publicly available ICEYE documentation (RD-1 – RD-5), together with documentation not publicly available but shared with the EDAP assessment team (RD-6 – RD-8), provided overall comprehensive information about the ICEYE products. The provided product details in RD-1 – RD-4 documents and in the metadata of the products themselves included all required information. The data is in a standard file format, easily read and understood. Data is also easily accessed and processed with the publicly available SNAP toolbox distributed by ESA. Data order and delivery to the customer was smooth due to well written and clear instructions regarding the FTP delivery procedures. Documentation describing the metrological traceability is not available. All relevant characteristics of the SAR system and data are provided, and metadata includes all relevant ancillary information. In addition to the basic Level 1 SAR products, ICEYE offers higher level products and solutions in various topics, including flood monitoring, vessel detection, agriculture, ice chart mapping for sea navigation and oil spill detection. Documentation describing these analyses can be accessed upon registration through ICEYE's web site.

Documentation about pre-flight calibration is minimal. The post launch data calibration and validation activities and uncertainty characterization performed by ICEYE are well documented. RD-5 – RD-8 provide a theoretical background on the analysed quality parameters and describe the analyses of the X4, X5 and X7 satellites performed by ICEYE. The IRF analyses assessing the spatial resolution and the side lobes are described in RD-6 for the X2-X5 satellites and in RD-8 for the X7 satellite. The geolocation accuracy assessment is presented in RD-7 for the X2-X5 satellites and in RD-8 for the X7 satellite. Methods and results of the radiometric accuracy assessment performed by ICEYE are presented in RD-5 for the X2-X5 satellites and in RD-8 for the X7 satellite. Methods for assessing the NESZ are not documented for X2-X5 but are included in the document describing the quality analysis on X7 (RD-8). At the time of writing this document, no documentation about calibration-validation activities of the X6 satellite was available. All relevant uncertainty values for SAR are provided, such as spatial resolution, ISLR, PSLR, NESZ and geolocation error. Single uncertainty values for the products are provided in the ICEYE web site and in the openly available documents RD-1 – RD-4, but more detailed information about the observed uncertainties is provided in documents RD-5 – RD-8. Pixel-wise uncertainty is not provided.

An independent assessment of the essential quality parameters in SAR, including spatial resolution, PSLR, ISLR, ENL, NESZ, AEP correction and radiometric stability was performed by FMI, using a representative dataset acquired with ICEYE's X4-X7 satellites from various test areas, including distributed target and point target sites. Only a few scenes of the X5 satellite were acquired before the satellite became inoperative, and therefore our analysis was concentrated on

the X4, X6 and X7 satellites. The measured quality parameters in our analyses were compared with the corresponding values stated by ICEYE. The validation was mainly performed using a SAR Quality Toolbox (SQT) developed by Aresys, dedicated for the assessment of SAR data quality (<https://www.aresys.it/end-to-end-simulation/>). Processing was also tested with the SNAP toolbox.

The measured quality parameters assessed in the IRF analysis performed over the corner reflector (CR) sites were generally in line with the values provided by ICEYE. The spatial resolution was mostly similar or even better than the provided values. The ISLR was typically within the expected range, but the PSLR was often somewhat higher (worse) than the provided values. Compared to other data providers of similar SAR data, the ICEYE products have generally higher spatial resolution, but also relatively high side lobes. This is because no smoothing window function (e.g. Taylor, Hanning, Hamming or Kaiser) is applied by ICEYE during data processing. The measured localization errors were in accordance with the values provided by ICEYE.

The measured NESZ was typically higher (worse) than the values provided in the ICEYE documentation. However, this might be related to a possible overestimation by the SQT, or to the relatively steep incidence angles offered by ICEYE; maximum of 30° for Strip and 35° for Spot acquisition modes, posing a challenge in finding very low backscatter targets. The ENL in the homogenous Glacier and Desert targets was very close to the ideal value of 1 for SLC data. In rainforests the ENL was lower than expected, but this might be related to the areas being not ideally homogeneous in the assessed high spatial resolution data of ~0.5-3 m. The AEP was well corrected by ICEYE for the SL and SLH products, except for relatively low backscatter in the near range end in the X6 and X7 data. However, for the wider SM images having a larger variation of the antenna elevation angle, the AEP correction was less successful. Linear decreasing or increasing trends in the gamma nought backscatter ( $\gamma^0$ ) profiles were found in many of the analysed scenes. The shape of the  $\gamma^0$  profile was sometimes parabolic, which could be related to inaccuracies in the AEP correction, but also to an increased radiometric noise level of the images. The radiometric stability of the observations over the rainforests was usually according to radiometric accuracy stated by ICEYE, with observed deviations of less than 1 dB from the most typically measured backscatter level. Generally, the higher resolution SL and SLH imaging modes showed better stability than the SM data, especially for the X4 satellite. An improvement in the radiometric stability was observed for the newer satellites and/or processor versions.

The ICEYE data was successfully processed in the publicly available SNAP toolbox. The processing steps included image subset, calibration, geometric correction, and speckle filtering. The localization errors measured against known locations in Helsinki were larger than expected, but these measured errors can also be influenced by the accuracy of the manual measurements, the used DEM, the reference data, and the ICEYE data processor in SNAP. Based on our evaluation results and in light of the quality values provided by ICEYE, we conclude that the quality of X4-X7 satellites is generally in a good agreement with the values stated by ICEYE.

### 1.1 Mission Quality Assessment Matrix

Product Information		Product Generation		Ancillary Information		Uncertainty Characterisation		Validation	
Product Details		Sensor Calibration & Characterisation Pre-Flight		Product Flags		Uncertainty Characterisation Method		Reference Data Representativeness	
Availability & Accessibility		Sensor Calibration & Characterisation Post-Launch		Ancillary Data		Uncertainty Sources Included		Reference Data Quality	
Product Format		Additional Processing				Uncertainty Values Provided		Validation Method	
User Documentation						Geolocation Uncertainty		Validation Results	
Metrological Traceability Documentation									

Key	
Not Assessed	
Not Assessable	
Basic	
Intermediate	
Good	
Excellent	
	Information Not Public

Figure 1 – Mission Product Quality Evaluation Matrix for the ICEYE X4-X7 satellites

## 2. MISSION ASSESSMENT OVERVIEW

### 2.1 Product Information

Product Details	
Product Name	<i>ICEYE_[sat. number]_[PPL]_[im. mode]_[id]_YYYYMMDDTHHmss,</i>  <i>where [sat. number] is the number of the ICEYE satellite; X4-X7. [PPL] is the processing level of the product; SLC or GRD. [im. mode] is the imaging mode; SC for ScanSAR, SM for Stripmap, SL for Spotlight and SLH for Spotlight High. [id] is typically a four-to-six-digit product identification number. YYYYMMDD and HHmss are the acquisition start date and time.</i>
Sensor Name	<i>X4-X7 were evaluated</i>
Sensor Type	<i>X-band SAR</i>
Mission Type	<i>Constellation – 3 satellites out of the constellation are evaluated</i>
Mission Orbit	<i>Sun Synchronous Polar Orbit</i>
Product Version Number	<i>The evaluated products are of processor versions 0.99- 1.43</i>
Product ID	<i>A number with four to six digits individual for each product</i>
Processing level of product	<i>Level 1 SLC products were evaluated</i>
Measured Quantity Name	<i>Radar Backscatter</i>
Measured Quantity Units	<i>dB</i>
Stated Measurement Quality	<i>Absolute radiometric accuracy, i.e. the RMSE (root mean square error) between the measured and the true RCS, is estimated &lt; 2 dB. The relative radiometric accuracy (standard deviation of the radiometric error of known targets within one data take) estimate is &lt; 1 dB for Strip data.</i>
Spatial Resolution (m)	<i>Spot, Strip and Scan acquisition modes are offered. The spatial resolution (range X azimuth) for each mode is: Scan: 15 x 15 (GRD) Strip: 0.5-2.5 x 3 (SLC) Spot: 0.5 x 0.25 (SLC)</i>
Spatial Coverage (km)	<i>Size of one standard scene (swath width x length) Scan: 100 x 100 Strip: 30 x 50 Spot: 5 x 5</i>
Temporal Resolution	<i>Daily repeat pass for selected targets (not yet global)</i>
Temporal Coverage	<i>The first ICEYE satellite was launched in January 2018. Constellation is continuously expanding</i>
Point of Contact	<a href="mailto:customer@iceye.com"><i>customer@iceye.com</i></a>
Product locator (DOI/URL)	<i>NA</i>
Conditions for access and use	<i>Data were provided under specific agreement for utilization within the EDAP framework.</i>
Limitations on public access	<i>NA</i>

Product Abstract	NA
------------------	----

Availability & Accessibility	
Compliant with FAIR principles	<i>Most of the Fair principles met, except: Metadata and data include qualified references to other (meta)data.</i>
Data Management Plan	<i>Standard orders are submitted via email to customer service, by filling out a Standard Order Form with required information on requested datasets. Custom orders with a higher level of flexibility are initiated by submitting a Custom Order Form via the email. Access to the public archive of ICEYE radar preview imagery is possible after registration.</i>
Availability Status	<i>Standard orders are delivered via SFTP server to the customer within 12 hours after the data is acquired. Faster delivery times are possible if near real-time data is required. Archive scenes are delivered up to 12 hours after an order is received. Possibility to use free software (e.g. SNAP) for data processing and analysis.</i>

Product Format	
Product File Format	<i>HDF5 and XML for SLC data GeoTIFF and XML for GRD data PNG and KML for quicklooks</i>
Metadata Conventions	<i>HDF, XML</i>
Analysis Ready Data?	<i>No</i>

User Documentation		
Document	Reference	QA4ECV Compliant
Product User Guide	<i>SAR Product Guide. Latest version available at: <a href="https://www.iceye.com/sar-data/documents">https://www.iceye.com/sar-data/documents</a> (11/2021)</i>	<i>No</i>
Product Format Specification	<i>Level 1 Product Format Speciation Document, version 2.1, released in 11/6/2020. Latest version available at: <a href="https://www.iceye.com/sar-data/documents">https://www.iceye.com/sar-data/documents</a> (11/2021)</i>	<i>No</i>
Data Calibration and Validation	<i>Data Calibration and Validation, version 1.0, released 22/6/2020. Contains Cal-Val analyses of X2-X5 satellites. Latest version available at: <a href="https://www.iceye.com/sar-data/documents">https://www.iceye.com/sar-data/documents</a> (11/2021)</i>	<i>No</i>

Metrological Traceability Documentation	
Document Reference	<i>Not available</i>
Traceability Chain / Uncertainty Tree Diagram Available	<i>No</i>

## 2.2 Product Generation

Sensor Calibration & Characterisation – Pre-Flight	
Summary	<i>All relevant characteristics of a SAR system stated. Documentation about pre-flight calibration is minimal.</i>
References	RD-1 RD-3

Sensor Calibration & Characterisation – Post-Launch	
Summary	<i>Metadata includes all reasonable aspects of the sensor characteristics. Post-launch calibration methods are well explained in the Data Calibration and Validation document (RD-5) for X2-X5 satellites, and in the Data Quality Assessment document for X7 (RD-8). The radiometric calibration was performed using homogeneous targets and point targets. It included e.g. antenna elevation beam calibration and calibration coefficient calculation. Calibration against homogeneous targets was initially performed over Amazon rainforest, and a validation of the calibration parameters was done using Congo rainforest data. The corner reflectors in Rosamond JPL site were used in the radiometric calibration against point targets. The calibration parameters were derived through an analysis of many images. Routine and ongoing validation activities are planned for the operational ICEYE satellites. Documents describing the calibration and validation performed for the X6 satellite were not available at the time of writing this report.</i>
References	RD-1 RD-3 RD-5 RD-8

Additional Processing	
Description	<i>Some Level-2 products and solutions are offered by ICEYE for different applications, such as flood monitoring, vessel detection, agriculture, ice chart mapping for sea navigation and oil spill detection. The development of Level-2 products is gradually increasing, as the number of satellites increase, and the calibration metrics evolve. Level-2 products were not evaluated within this work</i>
Reference	RD-3

## 2.3 Ancillary Information

Product Flags	
Product Flag Documentation	RD-3 RD-5 RD-8

Comprehensiveness of Flags	<i>Basic flags indicating if antenna elevation pattern compensation, free space loss compensation and windowing function were applied. Additional flags indicating the quality of the observations are not provided.</i>
----------------------------	--

Ancillary Data	
Ancillary Data Documentation	RD-3
Comprehensiveness of Data	<i>All the necessary and relevant ancillary data for SAR systems exist. There are no additional ancillary data related to ground conditions at the time of imaging, such as meteorological data.</i>
Uncertainty Quantified	No

## 2.4 Uncertainty Characterisation

Uncertainty Characterisation Method	
Summary	<i>The methods for uncertainty characterization are generally well documented. Methods describing the performed IRF analyses, including the assessment of spatial resolution and the side lobes are described in RD-6 for X2-X5, and in RD-8 for X7. Geolocation accuracy assessment performed by ICEYE is described in documents RD-7 for X2-X5 and in RD-8 for X7. Methods for assessing the radiometric accuracy are presented in RD-5 for X2-X4 and in RD-8 for X7. Methods for assessing the NESZ are documented only for X7 (RD-8). Documents describing the methods for uncertainty characterization of the X6 satellite were not available.</i>
Reference	RD-5 RD-6 RD-7 RD-8

Uncertainty Sources Included	
Summary	<i>The SAR processor compensates for the effects of range spread loss, elevation antenna pattern, different azimuth and range bandwidths, and sensor settings variations (receiver gain, transmit power, duty cycle)</i>
Reference	ICEYE web site RD-2 RD-8

Uncertainty Values Provided	
Summary	<i>All relevant uncertainty values for SAR are provided. The given uncertainty values are based on analyses of several datasets. Single uncertainty values for each imaging mode are provided in the ICEYE web site and in the openly available documentation. A more detailed description of uncertainty characterization performed by ICEYE for the satellites X4, X5 and X7 is provided in the additional documentation (some not openly available). Pixel-wise uncertainty is not provided.</i>
Reference	RD-1 RD-5 RD-6 RD-7 RD-8

Analysis Ready Data?	No
----------------------	----

Geolocation Uncertainty	
Summary	<i>One single typical geolocation uncertainty value of 10 m for all ICEYE standard products is given in the ICEYE web page (checked at 11/2021). In the newest SAR Product Guide the CEP90 geolocation error is given as a single value for each imaging mode separately (one value for all satellites), while in an older version of the SAR product guide the CEP90 is given as a single value for each satellite (for X2-X5 satellites). In the additional documentation (not publicly available) provided by ICEYE to the assessment team, the geolocation uncertainty is given in a more detailed manner. The Absolute Location Error, Root Mean Square Error, and Circular Error at the 90% percentile calculated with the three different methods are presented for several test acquisitions, in RD-7 for X2-X5 and in RD-8 for X7.</i>
Reference	ICEYE web page RD-2 RD-7 RD-8

## 2.5 Validation

Validation Activity #1	
Independently Assessed?	Yes
<i>Reference Data Representativeness</i>	
Summary	<i>Reference measurements assessed are well representative of the satellite measurements, covering a reasonable range of ICEYE's X4, X6 and X7 satellite's measurements. The number of assessed scenes is 45-50 per satellite, including images from corner reflector (CR) sites for the IRF and localization error analyses, as well as low backscatter images from water and desert areas, and images from homogenous targets in Amazonas rainforest and glaciers for radiometric analyses. The reference datasets enable an assessment of the most essential quality parameters in SAR, such as the spatial resolution, geolocation accuracy, PSLR, ISLR, ENL, NESZ, AEP and radiometric stability.</i>
Reference	Chapter 3
<i>Reference Data Quality &amp; Suitability</i>	
Summary	<i>The quality parameters of the reference data are usually given as single uncertainty values representing all datasets of the same acquisition mode (e.g. Spot, Strip). In the public documentation the provided quality values are more general, while in the not publicly available documentation provided to the EDAP assessment team, the quality values were presented in a more detailed manner.</i>
Reference	RD-1 – RD-8
<i>Validation Method</i>	
Summary	<i>The relevant quality parameters of SAR measured from the test datasets are compared with the uncertainty/quality values provided by ICEYE in their documentation. The validation was mainly performed using a dedicated SAR quality analysis toolbox (SQT), but processing was also tested with the SNAP toolbox. Dedicated test areas including CR sites, rainforests, glaciers, water, deserts, and sites with known targets were used for the evaluation.</i>

Reference	Chapter 3
<i>Validation Results</i>	
Summary	<p>A grading in the scale of Excellent, Good, Intermediate and Basic quality (as in the maturity matrix shown in section 1.1) is given below for each of the assessed SAR quality parameters, followed by a short explanation. See Chapter 3 for a more detailed description of the data quality analysis performed by FMI.</p> <ul style="list-style-type: none"> <li>• <b>Spatial resolution: Excellent</b> quality. <i>The spatial resolution of the test data was mostly similar or even better than the values provided by ICEYE.</i></li> <li>• <b>PSLR and ISLR: Intermediate</b> quality. <i>The ISLR was within the expected range, but the PSLR was sometimes higher (worse) than the values provided by ICEYE.</i></li> <li>• <b>Localization error: Good</b> quality. <i>The measured localization errors were typically smaller than the CEP90 localization error provided by ICEYE.</i></li> <li>• <b>NESZ: Basic</b> quality. <i>The measured NESZ was usually higher (worse) than the values provided by ICEYE. The strong NESZ could be caused by the relatively simple calculation method, or due to the difficulty in finding areas with very low backscatter due the relatively steep incidence angles available for the ICEYE data.</i></li> <li>• <b>ENL: Good</b> quality <i>The measured ENL in the Glacier and Desert sites was very close to the ideal value of ENL=1 for SLC product type, reflecting a correct radiometric distribution. The ENL in rainforests was too low, but this might be related to the difficulty in finding entirely homogeneous regions for the relatively high-resolution data.</i></li> <li>• <b>AEP correction: Basic</b> quality <i>The AEP correction performed by ICEYE was reasonable for the SL and SLH products, except in the near range end for X6 and X7 data, where the backscatter was relatively low. For the SM data having a larger variation of the antenna elevation angle, the AEP correction was less successful. Linear decreasing or increasing trends in the gamma nought backscatter (<math>\gamma^0</math>) profiles were found in many of the analysed scenes. The shape of the <math>\gamma^0</math> profile was sometimes parabolic, which could also be related to an increased radiometric noise level in the image.</i></li> <li>• <b>Radiometric stability: Good</b> quality <i>The average backscatter level in rainforests was typically within 1 dB from the most typical value, which is in accordance with the 2 dB RMSE radiometric accuracy derived by ICEYE in the commissioning phases. An improvement in the stability towards newer satellites and/or processor versions could be seen.</i></li> </ul>
Reference	Chapter 3

### 3. DETAILED ASSESSMENT

This chapter provides detailed information on the independent data analysis and evaluation performed by FMI using the test data from the X4, X6 and X7 ICEYE satellites. Evaluated data included Stripmap (SM), Spotlight (SL), and High Resolution Spotlight (SLH) scenes as SLC product type. All ICEYE data are in VV-polarization (single-polarization), with incidence angles ranging between 15 and 35 degrees. Data were collected from various test sites enabling a comprehensive assessment of the most relevant SAR quality metrics, such as spatial resolution, peak side lobe ratio (PSLR), integrated side lobe ratio (ISLR), geolocation accuracy, equivalent number of looks (ENL), noise equivalent sigma zero (NESZ), antenna elevation pattern (AEP), and radiometric stability. Table 1, Table 2 and Table 3 list the test areas, imaging modes, product ID numbers, acquisition dates and processor version numbers of the ICEYE scenes used by the evaluation team for assessment purposes within the EDAP activity, for X4, X6 and X7 satellites, respectively.

The data used for assessment includes scenes from distributed homogeneous and low backscatter areas, as well as point target test sites with known target locations. Data from Rainforest, Glacier, Doldrum and Desert areas were acquired for all three evaluated satellites: X4, X6 and X7. Rainforests and glaciers are considered homogeneous targets, and especially in rainforests the measured backscatter has low dependency on imaging angles. These test areas are used for evaluating the ENL, the AEP, and the radiometric stability. The Doldrums zone in the Atlantic and Pacific Oceans as well as smooth desert surfaces cause low backscatter, due to specular reflection of the radar signal on the smooth surfaces and high penetration in the dry sand (for desert). The low backscatter targets are used for assessing the NESZ.

IRF analyses are performed over dedicated sites with corner reflectors (CRs), providing quality values for spatial resolution, geolocation accuracy, and the power distribution of the measured radar beam (PSLR and ISLR). Suitable CR sites for the IRF analyses were selected based on the orbits and coverage of the individual satellites. Especially for X6 and X7 satellites, options for possible CR sites were very limited, due narrow spatial coverage selected by ICEYE for gaining short repeat pass times. Changing orbits of individual satellites also added complexity in finding suitable CR sites and planning the image acquisitions. Ideally, if possible, two different CR sites were chosen for each evaluated satellite. For X4, the Sodankylä airfield containing CRs managed by FMI, and the Rosamond CR array test site managed by JPL were selected. For X7, few archive scenes from the Rosamond CR site were available, and in addition, a CR located in Kiruna, Northern Sweden, was selected for the rest of the scenes required for the IRF analysis. For X6, only the Rosamond CR site was feasible, although the alignment of the CRs, designed primarily for right looking orbits, was not optimal for the ascending left looking orbit of X6 over the site. Nevertheless, the CRs were still well visible in the SAR images allowing a proper IRF analysis also for X6. Data from the Helsinki airport were acquired for X4 and X6 satellites for testing the compatibility of ICEYE data with the SNAP toolbox, and for further testing the geolocation accuracy against known targets.

Few X4 scenes were delivered to FMI during autumn 2019, and the rest of the X4 data were acquired and delivered between July 2020 and March 2021. Few X7 archive scenes acquired during the end of 2020 and the beginning of 2021 from Rosamond, together with new acquisitions acquired from the other test areas during spring and summer 2021 were delivered to FMI in May-August 2021. All X6 data were acquired and delivered to FMI during September-October 2021.

The SAR Quality Toolbox developed by Aresys was mainly used for assessing the above-mentioned quality metrics. The measured quality values were evaluated by comparing them to the corresponding quality values provided by ICEYE in the publicly available documentation and in the additional documentation not publicly available but provided by ICEYE to the EDAP assessment team. The evaluation results are therefore considered good if the measured quality parameters are better or similar than the values provided by ICEYE. On the contrary, the quality is considered weak if the measured quality parameters are worse than the provided values in the documents. In spring 2020 ICEYE decided on providing SLH instead of the SL imaging mode (with the same price), and the name of the SLH imaging mode was changed to Spot. Hence, in the most recent ICEYE

documentation and in the ICEYE web site, quality values for the old SL mode are not shown. Quality values provided by ICEYE for the SL mode are therefore taken from previous versions of the ICEYE documentation.

**Table 1: X4 data products provided by ICEYE to FMI and included in the data analysis and evaluation.**

Test Area	Imaging mode	ID number	Date	Version number	
Point targets with known location	SM	38152	20201125	1.22	
		38153	20201219	1.24	
		38154	20210112	1.24	
	SL	38155	20201124	1.21	
		41488	20210207	1.26	
		45277	20210302	1.26	
	SLH	38156	20201218	1.24	
		38565	20210206	1.26	
		45599	20210303	1.26	
	Sodankylä, Finland	SM	9939	20190920	0.99
			34001	20200822	1.16
			34055	20201009	1.17
		SL	34002	20200823	1.16
			34004	20200916	1.16
			36138	20201101	1.18
SLH	34054	20201008	1.17		
	34056	20200915	1.16		
	36139	20201102	1.31		
Helsinki Airport	SM	36144	20201017	1.17	
		36147	20201019	1.17	
	SL	36142	20201016	1.17	
SLH	36150	20201111	1.19		
	36143	20201016	1.17		
	36145	20201107	1.19		
Low backscatter water or desert	SM	33037	20200726	1.14	
		33039	20200726	1.14	
	SL	33032	20200730	1.14	
		33033	20200731	1.15	
	SM	33044	20200726	1.14	
		33045	20200727	1.14	
	SL	33040	20200726	1.14	
		33041	20200727	1.14	
	SM	38554	20201209	1.24	
38555		20201220	1.24		
SL	38552	20201219	1.24		
	38631	20201226	1.24		
Homogeneous areas	SM	10014	20190919	0.99	
		38638	20201207	1.22	
		38639	20201209	1.24	
		38640	20201211	1.24	
	SL	38159	20201203	1.22	
		38160	20201205	1.22	
		38641	20201208	1.24	
		38642	20201212	1.24	
	SM	38561	20201204	1.22	
		38674	20201207	1.22	
SL	38563	20201204	1.22		
	38564	20201204	1.22		

**Table 2: X6 data products provided by ICEYE to FMI and included in the data analysis and evaluation.**

Test Area	Imaging mode	ID number	Date	Version number
<b>Point targets with known location</b>	SM	130582	20210908	1.40
		132642	20210925	1.41
		132643	20210926	1.41
		132645	20210927	1.41
		132646	20210928	1.41
		132648	20210929	1.41
		132649	20210930	1.41
		132650	20211001	1.42
		132651	20211002	1.41
		137634	20211004	1.41
	SLH	130583	20210909	1.40
		132627	20210916	1.40
		132628	20210917	1.40
		132630	20210918	1.40
		132631	20210919	1.40
		132637	20210921	1.41
		132638	20210922	1.41
		132639	20210923	1.41
		132656	20210915	1.40
		137317	20211003	1.42
Helsinki Airport	SM	137630	20210925	1.41
		137631	20210926	1.41
	SLH	137632	20210927	1.41
		137633	20210928	1.41
<b>Low backscatter water or desert</b>	SM	129957	20210904	1.40
		129959	20210905	1.40
	SLH	129810	20210902	1.40
		129813	20210904	1.40
	SM	132461	20210914	1.40
		132475	20210915	1.40
	SLH	129811	20210902	1.40
		129812	20210903	1.40
Desert, Sahara	SM	137310	20210925	1.41
		137316	20210930	1.41
	SLH	137302	20210923	1.41
		137313	20210927	1.41
<b>Homogeneous areas</b>	SM	130568	20210908	1.40
		130569	20210909	1.40
		130579	20210910	1.40
		132661	20210916	1.40
	SLH	130571	20210911	1.40
		130572	20210912	1.40
		132663	20210917	1.40
		132664	20210918	1.40
Glacier, Antarctica	SM	129956	20210904	1.40
		132489	20210914	1.40
	SLH	129954	20210903	1.40
		129955	20210904	1.40

**Table 3: X7 data products provided by ICEYE to FMI and included in the data analysis and evaluation.**

Test Area		Imaging mode	ID number	Date	Version number
<b>Point targets with known location</b>	Rosamond, California	SL	39540	20201229	1.24
		SLH	37548	20201111	1.20
			39557	20201230	1.33
			39573	20201231	1.33
			42795	20210216	1.33
	Kiruna, Sweden	SM	92582	20210804	1.36
			103507	20210815	1.36
			103510	20210816	1.36
			103512	20210817	1.36
			103513	20210818	1.36
			103516	20210819	1.36
			103519	20210820	1.36
		140212	20211001	1.41	
		SLH	90943	20210803	1.36
			95409	20210806	1.36
			98201	20210807	1.36
			99515	20210808	1.36
			100835	20210809	1.36
			103490	20210811	1.36
	103496		20210812	1.36	
103499	20210813	1.36			
103503	20210814	1.36			
111359	20210821	1.36			
114401	20210822	1.36			
140691	20210930	1.41			
<b>Low backscatter water or desert</b>	Doldrums, Atlantic	SM	58358	20210703	1.43
		58360	20210706	1.43	
	SLH	67166	20210708	1.43	
		67901	20210709	1.43	
	Doldrums, Pacific	SM	58359	20210705	1.43
		58363	20210709	1.43	
	SLH	98795	20210807	1.43	
		103086	20210810	1.43	
Desert, Sahara	SM	58370	20210530	1.43	
	58371	20210531	1.43		
SLH	58369	20210528	1.43		
	58864	20210529	1.43		
<b>Homogeneous areas</b>	Rainforest, Amazon	SM	58352	20210529	1.41
			58356	20210531	1.41
		SLH	58813	20210603	1.41
			58946	20210528	1.41
	SLH	58350	20210528	1.41	
		58351	20210529	1.41	
		58353	20210530	1.41	
		58354	20210531	1.41	
	Glacier, Antarctica	SM	59211	20210601	1.41
		59292	20210602	1.41	
SLH	58812	20210531	1.41		
	58838	20210531	1.41		

### 3.1 IRF Analysis

An IRF analysis is performed on the scenes with CRs, assessing the spatial resolution, the ratio of the secondary lobes with the main lobe, and the geolocation accuracy of the SAR scenes. Three different test areas containing CRs were selected for the IRF analysis: The Rosamond Corner Reflector Array calibration site in California, USA, managed by JPL (Figure 2), the Sodankylä airfield site located in Northern Finland managed by FMI (Figure 3, Figure 4), and Kiruna in Northern Sweden managed by the Swedish Space Corporation (Figure 3).

The Rosamond site contains several trihedral CRs with face widths of 4.8 m, 2.4 m, and 0.7 m. Most of the reflectors are directed towards the east (descending right looking orbits), including all large (4.8 m), all small (0.7 m) and part of the medium size (2.4 m) reflectors. The Sodankylä airfield site contained 6 trihedral CRs in 2019 and 4 trihedral CRs in 2020, all of them with a face width size of 0.9 m and aligned with the satellite imaging geometry. The Kiruna site contained two trihedral CRs reflector with face widths of 3.8 m, one pointed to ascending and the other to descending right looking orbits. Only one CR was thus visible in the ICEYE SAR scenes.

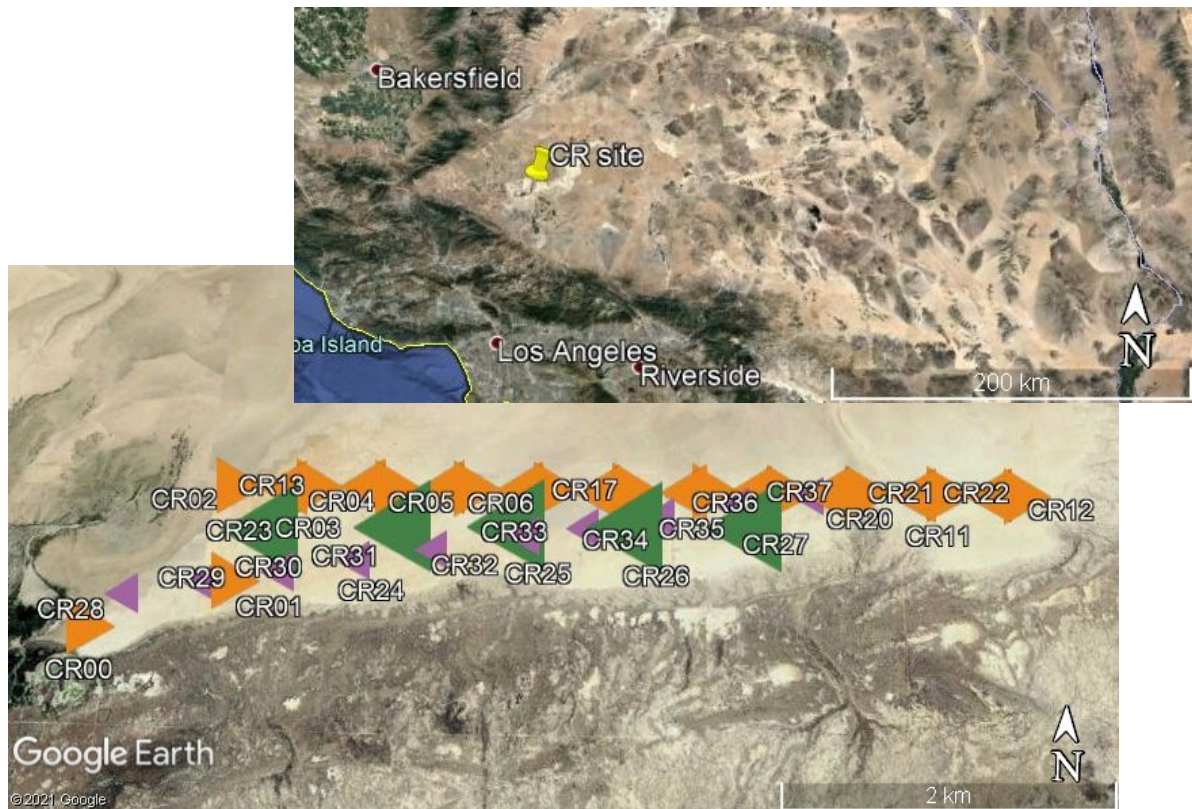


**Figure 2: A Google Earth view of the Rosamond CR site in California. The smaller image in the upper right side is a zoom out showing the surrounding area of the CR site. The bottom image is a zoom in on the CR site, showing the CR names, alignment, and distribution at the site.**

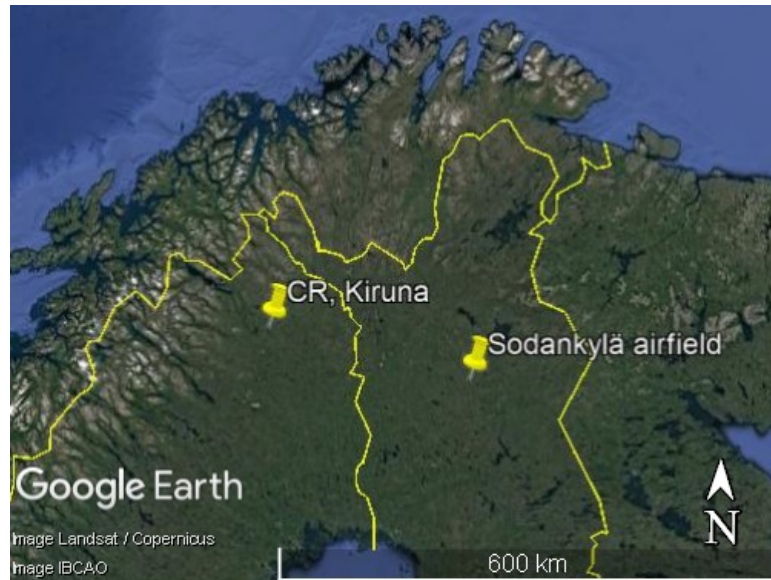


Figure 3: The Sodankylä airfield and Kiruna test sites marked on Google Earth satellite view.

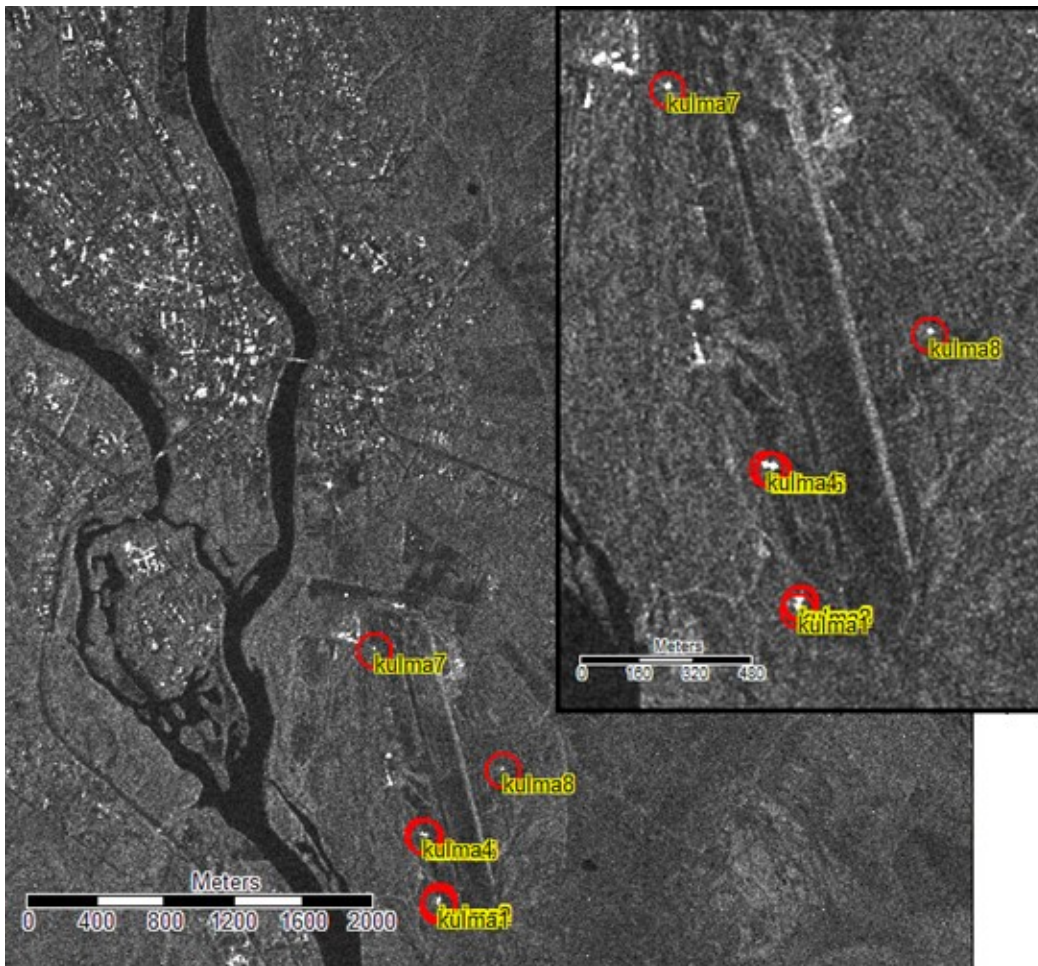
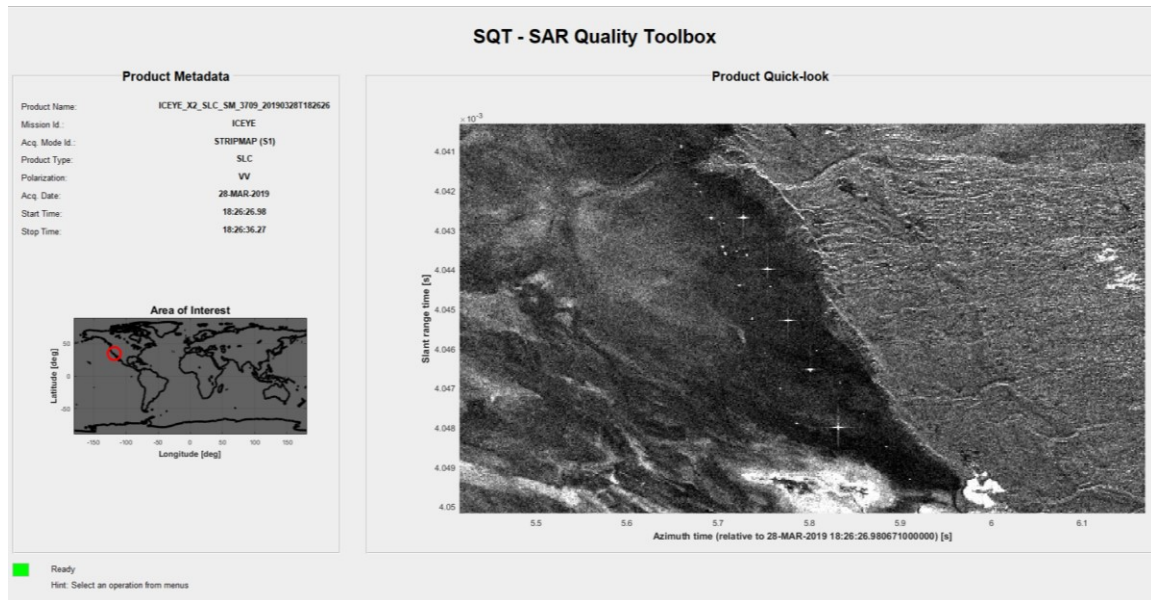
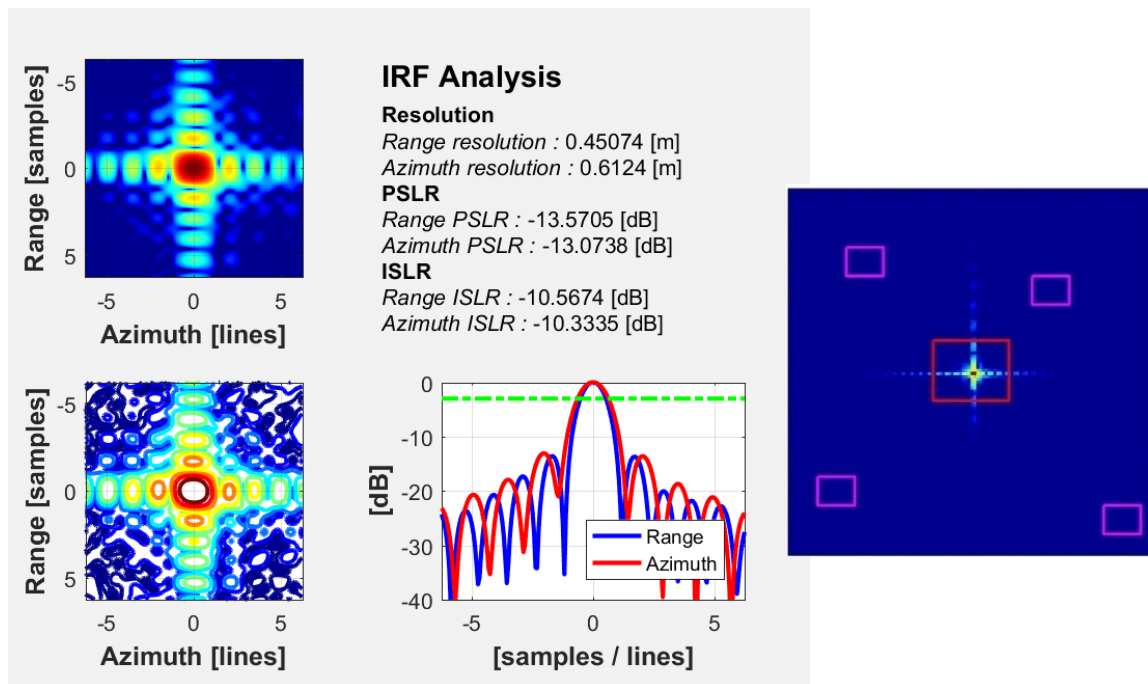


Figure 4: The Sodankylä airfield CR site observed by the ICEYE satellite. The large image shows the airfield, which is located south-east from the town of Sodankylä, and the smaller image in the upper right side is a zoom in on the airfield, showing the CR's as bright dots on the SAR image.

The IRF analysis is performed using the SQT software of Aresys, specifically designed for quality analysis of various SAR data. The distribution of the measured power from the reflectors and the area around the reflectors are analysed, providing the spatial resolution of the SAR data and the power of the secondary lobes relative to the main lobe (PSLR and ISLR). The individual CRs are first located automatically by the SQT or by manually selecting specific CRs, and the IRF parameters are then calculated by the software for the included CRs. A screenshot showing an example of an IRF analysis in the SQT for Rosamond is shown in Figure 5. The bright points in the image are the reflectors as observed by the SAR scene. Figure 6 shows an example of the spatial distribution of the measured power from one of the CRs in Rosamond and the obtained results for the spatial resolution, PSLR and ISLR.



**Figure 5: IRF analysis in Rosamond, California, using the SQT. White dots inside the relatively dark area in the middle of the image are CRs as seen in a SAR image.**



**Figure 6: Assessment of the spatial resolution, PSLR and ISLR for the X4 SL scene 41488 from Rosamond on the left. RCS of one CR, observed by the SL 38155 scene from Rosamond on the right.**

The IRF analysis typically includes a calculation of the localization error of a SAR scene. The given locations of the bright targets (CRs) are compared with the locations of the CRs in the SAR image. The localization error is expressed in both azimuth and range directions. An option for manual IRF analysis is available along with an automated analysis in which the SQT generates a HTML report showing the results. Figure 7 presents the results of a manual analysis of an example CR over Rosamond, for ICEYE X4 Spotlight images 41488 and 38155. The red dot is the expected location of the reflector on the SAR image, based on the geographical coordinates of the reflector (e.g. the true location). The green plus (+) sign shows the location of the same reflector on the SAR image, calculated by the software based on the backscatter distribution.

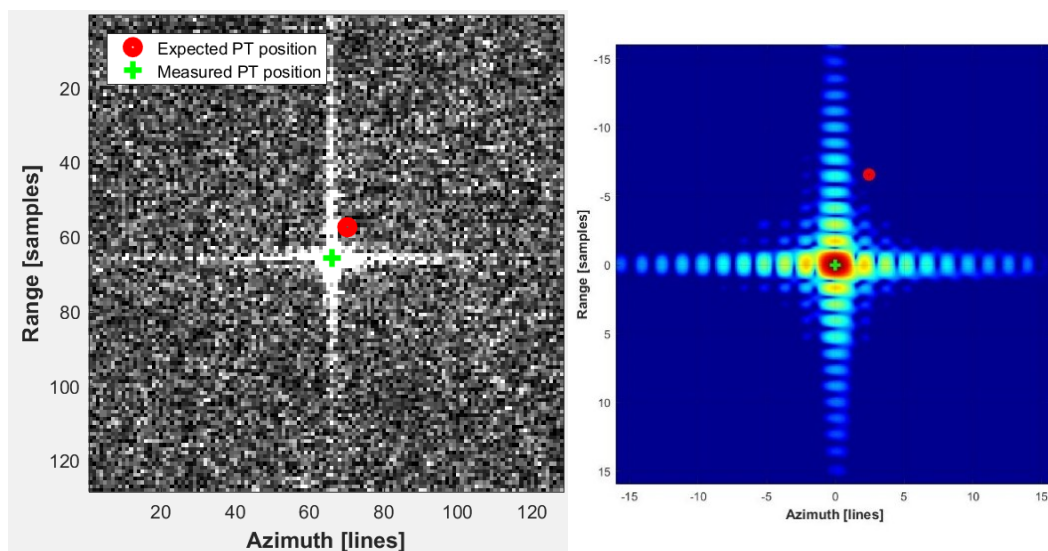


**Figure 7. Geolocation accuracy assessment with the SQT. The expected point target (red dot) location is compared with the location in the observed SAR image (green plus sign). The examples above are from X4 SL scenes 41488 on the left and 38155 on the right side, both acquired from Rosamond.**

Table 4 shows the quality values related to the IRF analysis provided in the ICEYE documentation or in the ICEYE web site (checked 11/2021). The range spatial resolution is given in slant range direction for the assessed SLC data. The spatial resolution is given for each imaging mode separately. A single quality value of the PSLR and localization uncertainty is provided by ICEYE for all imaging modes. A value for the ISLR is not currently provided by ICEYE in the public documentation. In the previous version of the Product Guide an ISLR of approximately -4.4 dB was defined by ICEYE, but in the more recent analyses performed by ICEYE, the measured ISLR was mostly between -12 and -10 dB. Therefore, the reference ISLR concerning the EDAP evaluation activity is defined in Table 4 as between -12 and -4.4 dB. The CEP90 localization error provided in the most recent ICEYE product guide is 9 m for the Strip and Spot imaging modes. In our analysis we calculated the localization errors in range and azimuth directions for each scene, which can be considered the typical localization error values of the test data sets. It is therefore expected that at least 9 out of 10 scenes should have an absolute localization error (ALE) smaller than 9 m. The ALE is the Euclidian distance composed of the range and the azimuth errors.

**Table 4: Quality values of the test dataset related to the IRF analysis, provided in the ICEYE documentation.**

Product type	Range resolution [m]	Azimuth resolution [m]	PSLR [dB]	ISLR [dB]	Localization error [m]
Stripmap	0.5...2.5	3	-13.3	-12...-4.4	9...10
Spotlight	0.5	0.5			
HR Spotlight	0.5	0.25			

### 3.1.1 X4

Table 5 and Table 6 list the results of the IRF analysis performed for the ICEYE X4 satellite over the Rosamond and the Sodankylä airfield sites. The average and std of all included CRs are shown.

The measured slant range resolution in Rosamond and Sodankylä was typically around 0.47 m in SLH, 0.45 m in SL and 0.9-1.8 m in SM, with one exceptional SL scene showing 0.56 m spatial resolution. The range resolution was thus close or even better than the provided values. The measured azimuth resolution was typically around 0.24 m for SLH, 0.6-0.8 m for SL and 2.2-2.3 m for SM. For the SLH and SM modes the measured azimuth resolutions were thus better than the provided values, but for the SL mode they were somewhat coarser. Overall, the measured spatial resolution of the X4 data from Rosamond and Sodankylä was in line with the values provided in the ICEYE documentation.

The PSLR in range and azimuth directions was between -17 and -12 dB for the SLH mode, between -14 and -12 dB for SL, and between -15 and -9 dB for the SM mode. The measured ISLR in range and azimuth directions was between -15 and -9 for SLH, between -11 and -9 for SL, and between -12 and -9 dB for SM imaging modes, all within or slightly weaker (better) than the reference ISLR values in Table 4. As an exception for the values mentioned above, SL 45277 from Rosamond showed exceptionally strong PSLR and ISLR, indicating a possible problem in data processing or calculation of the side lobes by the software. Also, scenes SM 9939 and SM 34055 from Sodankylä showed somewhat stronger range ISLR values. Generally, the measured PSLR was often stronger than the values provided by ICEYE, and the measured ISLR was within the range of the expected values.

The measured localization errors were generally larger in Sodankylä than in Rosamond, especially in the range direction. In Rosamond the ALE was always less than 7 m, but in Sodankylä it was between 11 and 18 m. The constant negative shift of 8-18 m in range direction in Sodankylä suggests that there could have been a bias in the GPS measurements of the CR locations. If shifting the measured location in range direction for 12 m for all scenes, the ALE would be similar to what

was observed in Rosamond. Therefore, overall, the localization accuracy of the X4 data can be considered in line with the values provided by ICEYE.

**Table 5. Rosamond IRF analysis for X4; average and std of all included CRs.**

Image ID	Range resolution [m]	Azimuth resolution [m]	Range PSLR [dB]	Azimuth PSLR [dB]	Range ISLR [dB]	Azimuth ISLR [dB]	Range Location Error [m]	Azimuth Location Error [m]
SL_38155	0.46 ± 0.017	0.70 ± 0.012	-13.24 ± 1.013	-12.40 ± 0.995	-9.73 ± 1.670	-9.33 ± 1.439	2.80 ± 0.034	-1.28 ± 0.071
SL_41488	0.45 ± 0.003	0.61 ± 0.003	-13.63 ± 0.313	-13.00 ± 0.425	-10.50 ± 0.449	-10.06 ± 0.700	3.57 ± 0.034	-2.02 ± 0.041
SL_45277	0.56 ± 0.291	0.88 ± 0.281	-5.37 ± 2.032	-4.93 ± 2.062	1.89 ± 1.880	1.89 ± 1.778	0.88 ± 14.026	1.70 ± 21.660
SLH_38156	0.50 ± 0.007	0.28 ± 0.009	-16.95 ± 1.812	-15.28 ± 1.839	-13.98 ± 2.704	-13.24 ± 2.659	2.49 ± 0.053	-1.60 ± 0.042
SLH_38565	0.45 ± 0.002	0.22 ± 0.004	-13.36 ± 0.354	-12.42 ± 1.069	-10.33 ± 0.313	-9.94 ± 0.882	3.06 ± 0.046	-2.48 ± 0.027
SLH_45999	0.45 ± 0.003	0.22 ± 0.009	-13.33 ± 0.551	-12.17 ± 0.674	-10.23 ± 0.462	-9.81 ± 0.568	3.38 ± 0.047	-2.20 ± 0.099
SM_38152	0.88 ± 0.014	2.17 ± 0.024	-12.89 ± 0.819	-14.48 ± 1.219	-9.55 ± 1.167	-11.42 ± 1.586	1.83 ± 10.163	-2.72 ± 5.954
SM_38153	0.97 ± 0.009	2.19 ± 0.026	-12.75 ± 1.053	-14.69 ± 0.764	-9.49 ± 1.528	-11.34 ± 1.726	-0.90 ± 13.238	-6.71 ± 18.500
SM_38154	1.12 ± 0.024	2.32 ± 0.046	-12.26 ± 1.725	-14.16 ± 1.399	-9.02 ± 2.180	-10.62 ± 2.780	-0.98 ± 15.151	-6.18 ± 20.004

**Table 6. Sodankylä IRF analysis for X4; average and std of all included CRs.**

Image ID	Range resolution [m]	Azimuth resolution [m]	Range PSLR [dB]	Azimuth PSLR [dB]	Range ISLR [dB]	Azimuth ISLR [dB]	Range Location Error [m]	Azimuth Location Error [m]
SL_34002	0.45 ± 0.001	0.67 ± 0.004	-13.21 ± 0.368	-13.36 ± 0.189	-10.51 ± 0.259	-10.20 ± 0.468	-13.54 ± 5.584	5.56 ± 3.678
SL_34004	0.45 ± 0.001	0.67 ± 0.001	-13.50 ± 0.090	-13.31 ± 0.136	-10.50 ± 0.094	-10.44 ± 0.073	-11.63 ± 0.098	-1.58 ± 0.100
SL_36138	0.46 ± 0.005	0.61 ± 0.003	-12.44 ± 0.826	-13.46 ± 0.349	-10.21 ± 0.153	-10.30 ± 0.152	-14.60 ± 0.048	0.18 ± 0.105
SLH_34054	0.50 ± 0.002	0.24 ± 0.001	-16.93 ± 0.462	-13.39 ± 0.208	-14.99 ± 0.276	-10.96 ± 0.157	-14.03 ± 0.071	-0.83 ± 0.110
SLH_34056	0.49 ± 0.003	0.24 ± 0.001	-16.50 ± 0.385	-13.51 ± 0.576	-14.59 ± 0.305	-11.01 ± 0.302	-11.10 ± 0.084	4.84 ± 0.108
SLH_36139	0.46 ± 0.014	0.23 ± 0.001	-12.31 ± 1.148	-12.49 ± 0.359	-10.54 ± 1.364	-9.95 ± 0.191	-16.57 ± 4.188	0.03 ± 0.476
SM_9939	1.83 ± 1.265	2.36 ± 0.016	-8.92 ± 7.315	-11.23 ± 0.770	-5.20 ± 7.438	-8.93 ± 0.581	-7.79 ± 8.019	9.84 ± 6.586
SM_34001	0.78 ± 0.006	2.25 ± 0.005	-12.62 ± 0.588	-15.17 ± 0.673	-9.98 ± 0.242	-12.07 ± 0.261	-18.05 ± 4.812	2.54 ± 3.851
SM_34055	1.07 ± 0.409	2.33 ± 0.026	-9.57 ± 5.332	-14.44 ± 0.099	-7.41 ± 4.441	-11.44 ± 0.189	-11.63 ± 0.070	-1.63 ± 0.104

### 3.1.2 X6

Table 7 lists the results of the IRF analysis performed for the ICEYE X6 satellite over the Rosamond CR sites. The average and std of all included CRs are shown. The measured slant range and azimuth resolution was very similar for all acquired X6 scenes over Rosamond. The measured

range resolution was 0.46 m in SLH and 0.91 m in SM, and the measured azimuth resolution was 0.23 m for SLH and around 2.18 m for SM. Overall, the measured spatial resolution of the X6 data from Rosamond was thus within or better than the values provided in the ICEYE documentation.

The PSLR in range and azimuth directions was between -13 and -11 dB for the SLH mode and between -15 and -9 dB for the SM mode. Except for the measured azimuth PSLR of SM, almost all measured values were thus stronger than the value of -13.3 dB provided in the documentation. The measured ISLR in range and azimuth directions was between -11 and -9 for SLH and between -12 and -9 dB for SM imaging modes, all within the reference ISLR values (Table 4). Generally, the measured PSLR was usually somewhat stronger than the values provided by ICEYE, and the measured ISLR was within the values provided and measured by ICEYE.

The ALE of the X6 scenes in Rosamond was typically less than 4 m. There were two Strip scenes with very large localization error: 132650 and 132651. The large errors are most likely caused by specific problems in data processing. Overall, the X6 test data is therefore in line with the values provided in the ICEYE documentation.

**Table 7: Rosamond IRF analysis for X6; average and std of all included CRs.**

Image ID	Range Resolution (m)	Azimuth Resolution (m)	PSLR Range (dB)	PSLR Azimuth (dB)	ISLR Range (dB)	ISLR Azimuth (dB)	Range Location Error (m)	Azimuth Location Error (m)
SLH_132656	0.46 ± 0.005	0.23 ± 0.007	-13.10 ± 0.363	-12.79 ± 0.867	-10.42 ± 0.335	-10.36 ± 0.828	1.75 ± 0.03	-0.45 ± 0.08
SLH_132639	0.46 ± 0.007	0.23 ± 0.006	-13.04 ± 0.517	-12.67 ± 1.318	-10.39 ± 0.393	-10.20 ± 1.349	2.81 ± 0.03	-2.37 ± 0.045
SLH_132638	0.46 ± 0.009	0.23 ± 0.005	-12.90 ± 0.375	-11.28 ± 1.217	-10.23 ± 0.388	-9.41 ± 1.156	2.95 ± 0.031	-0.80 ± 0.049
SLH_132637	0.46 ± 0.008	0.23 ± 0.005	-12.87 ± 0.327	-11.69 ± 0.997	-10.19 ± 0.506	-9.98 ± 1.08	2.33 ± 0.031	-0.68 ± 0.046
SLH_132631	0.46 ± 0.009	0.23 ± 0.008	-12.90 ± 0.378	-12.49 ± 1.033	-10.35 ± 0.582	-10.29 ± 0.614	3.22 ± 0.03	-0.51 ± 0.042
SLH_132630	0.46 ± 0.006	0.23 ± 0.008	-12.93 ± 0.242	-13.01 ± 0.903	-10.31 ± 0.395	-10.35 ± 0.747	2.84 ± 0.03	0.02 ± 0.043
SLH_132628	0.46 ± 0.007	0.23 ± 0.007	-12.83 ± 0.454	-13.50 ± 0.813	-10.32 ± 0.466	-10.73 ± 0.772	2.08 ± 0.03	0.23 ± 0.058
SLH_132627	0.46 ± 0.007	0.23 ± 0.007	-13.04 ± 0.469	-12.64 ± 1.32	-10.25 ± 0.403	-10.23 ± 1.031	2.38 ± 0.029	0.15 ± 0.079
SLH_130583	0.46 ± 0.007	0.23 ± 0.007	-12.79 ± 0.419	-11.29 ± 1.685	-10.18 ± 0.301	-9.20 ± 1.326	3.27 ± 0.027	-0.01 ± 0.067
SLH_137317	0.46 ± 0.008	0.23 ± 0.006	-12.89 ± 0.321	-12.24 ± 1.189	-10.19 ± 0.476	-9.85 ± 1.274	2.73 ± 0.028	-1.66 ± 0.053
SLH_137635	0.46 ± 0.009	0.23 ± 0.007	-12.88 ± 0.311	-11.71 ± 1.151	-10.24 ± 0.48	-9.82 ± 1.329	2.88 ± 0.037	-0.91 ± 0.07
SM_132642	0.91 ± 0.005	2.19 ± 0.009	-11.81 ± 0.4	-14.61 ± 0.288	-9.60 ± 0.397	-11.71 ± 0.398	4.15 ± 0.031	-1.59 ± 0.061
SM_130582	0.90 ± 0.01	2.13 ± 0.015	-11.91 ± 0.439	-14.52 ± 0.522	-9.44 ± 0.927	-11.67 ± 0.871	6.40 ± 0.03	2.47 ± 0.068
SM_132645	0.91 ± 0.005	2.19 ± 0.014	-11.86 ± 0.282	-14.38 ± 0.51	-9.74 ± 0.204	-11.74 ± 0.342	2.55 ± 0.032	-2.54 ± 0.058
SM_132643	0.91 ± 0.005	2.19 ± 0.009	-11.71 ± 0.271	-14.49 ± 0.409	-9.58 ± 0.378	-11.61 ± 0.51	3.62 ± 0.032	-3.50 ± 0.057
SM_132646	0.91 ± 0.004	2.19 ± 0.019	-11.87 ± 0.317	-14.59 ± 0.687	-9.57 ± 0.236	-11.62 ± 0.563	3.09 ± 0.032	-2.16 ± 0.069
SM_132648	0.91 ± 0.006	2.18 ± 0.021	-11.92 ± 0.533	-14.5 ± 0.649	-9.68 ± 0.341	-11.67 ± 0.485	3.85 ± 0.038	-1.70 ± 0.068
SM_132649	0.91 ± 0.006	2.19 ± 0.011	-11.91 ± 0.376	-14.57 ± 0.343	-9.68 ± 0.329	-11.70 ± 0.453	2.99 ± 0.037	-2.41 ± 0.058

SM_132650	0.92 ± 0.019	2.19 ± 0.023	-11.83 ± 0.589	-14.30 ± 1.522	-9.43 ± 1.023	-11.35 ± 1.991	8.79 ± 10.768	49.27 ± 4.738
SM_132651	0.91 ± 0.008	2.18 ± 0.015	-11.97 ± 0.337	-14.64 ± 0.269	-9.72 ± 0.254	-11.74 ± 0.513	11.19 ± 11.018	18.24 ± 4.837
SM_137634	0.91 ± 0.004	2.17 ± 0.014	-11.80 ± 0.35	-14.45 ± 0.659	-9.56 ± 0.333	-11.63 ± 0.65	4.81 ± 0.044	-0.49 ± 0.049

### 3.1.3 X7

Table 8 and Table 9 list the results of the IRF analysis performed for the ICEYE X7 satellite over the Kiruna CR and the Rosamond site. The average and std of all included CRs are shown in Table 9. At the time of image ordering, due to the narrow orbit of X7, Kiruna was the only relevant CR site available. The scenes from Rosamond are previously acquired SAR scenes ordered from the ICEYE image archive. The Kiruna site contained only one CR pointing towards the X7 orbit, and therefore, in order to have a sufficient number of samples, the number of ordered images was larger compared to the IRF analyses of X4 and X6.

The measured slant range resolution in Kiruna and Rosamond was always very close to 0.45 m in SLH, except for two scenes in Rosamond with values higher than 0.5. The range resolution in the one SL scene from Rosamond was 0.46 m, and the measured range resolution of the Kiruna SM scenes was always very close to 1 m. The measured azimuth resolution of the SLH mode was 0.22-0.24 m in all Kiruna scenes and around 0.24 m in Rosamond. The measured azimuth resolution of the one SL scene over Rosamond was 0.64 and of the SM scenes in Kiruna typically 2.3 m. Overall, the measured spatial resolution of the X7 data from Kiruna and Rosamond was thus in line or better than the values provided in the ICEYE documentation, with somewhat better quality over Kiruna than over Rosamond. The improvement seen in Kiruna can be related to the more recently acquired data, processed using a newer processor version (Table 3).

The measured PSLR in range and azimuth directions was usually between -14 and -12 dB for the SLH scenes from Kiruna and Rosamond and the one SL scene from Rosamond, and between -15 and -13 dB for the SM scenes of Kiruna. These values are mostly in line with the PSLR value provided by ICEYE. The measured ISLR in range and azimuth directions was usually between -11 and -9 for the SLH scenes from Kiruna and Rosamond and the one SL scene from Rosamond, and between -12.5 and -10 for the SM scenes of Kiruna. These values are in line with the ISLR value provided and measured by ICEYE. The ALE of the X7 scenes in Kiruna and Rosamond was typically less than 7 m. The localization error in the test datasets is therefore in line with the values provided by ICEYE.

**Table 8. Kiruna IRF analysis for X7.**

Image ID	Range resolution [m]	Azimuth resolution [m]	Range PSLR [dB]	Azimuth PSLR [dB]	Range ISLR [dB]	Azimuth ISLR [dB]	Range Location Error [m]	Azimuth Location Error [m]
SLH_90943	0.45176	0.22057	-13.5353	-12.5258	-10.4022	-9.6099	3.7981	-5.8452
SLH_95409	0.44866	0.22109	-13.7078	-12.5228	-10.4675	-29.9434	2.9705	-5.8602
SLH_98201	0.44828	0.22096	-13.6139	-12.1566	-10.4657	-9.8939	2.0231	-6.7694
SLH_99515	0.44884	0.22112	-13.6335	-12.7862	-10.4578	-9.9801	2.8246	-6.5654
SLH_100835	0.44848	0.22153	-13.5544	-11.4614	-10.4652	-9.768	2.3106	-6.0156
SLH_103490	0.45034	0.22072	-13.5636	-11.9032	-10.4019	-9.8915	3.4317	-5.4723
SLH_103496	0.44963	0.22168	-13.4745	-12.7791	-10.4457	-10.1121	2.7977	-5.9563
SLH_103499	0.4515	0.22053	-13.3726	-10.8812	-10.3916	-9.5211	3.1854	-6.0945
SLH_103503	0.4525	0.22032	-13.3858	-11.7266	-10.4679	-9.7767	2.6228	-5.9043
SLH_111359	0.45092	0.22106	-13.5311	-12.6526	-10.4366	-9.971	3.3675	-5.8525
SLH_114401	0.44816	0.22154	-13.5559	-12.3559	-10.4823	-10.0774	3.4677	-5.8053

SLH_140691	0,45244	0,23897	-13,4248	-12,8019	-10,4386	-9,9332	3,369	-5,4202
SM_92582	1.0087	2.3069	-12.9699	-15.0493	-10.1361	-12.3451	3.4987	-5.7482
SM_103507	1.0099	2.2948	-12.9103	-14.9959	-10.1987	-12.2281	3.2647	-5.688
SM_103510	1.0108	2.292	-12.9732	-14.9131	-10.2421	-12.2239	3.8624	-5.7791
SM_103512	1.009	2.2883	-12.9321	-14.9556	-10.1668	-12.2024	3.2661	-6.08
SM_103513	1.0082	2.2895	-13.0275	-14.8825	-10.1238	-12.2091	4.1103	-5.8733
SM_103516	1.0056	2.2895	-12.9058	-14.9846	-10.0058	-12.193	7.3759	-2.722
SM_103519	1.0198	2.2881	-12.6778	-14.9989	-9.9066	-12.2405	4.4281	-5.4838
SM_140212	1,0445	2,2585	-12,9283	-14,8924	-10,3103	-12,2762	4,1287	-5,4529

Table 9: Rosamond IRF analysis for X7; average and std of all included CRs.

Image ID	Range resolution [m]	Azimuth resolution [m]	Range PSLR [dB]	Azimuth PSLR [dB]	Range ISLR [dB]	Azimuth ISLR [dB]	Range Location Error [m]	Azimuth Location Error [m]
SL_39540	0.46 ± 0.006	0.64 ± 0.008	-13.84 ± 0.55	-12.70 ± 0.73	-10.65 ± 0.839	-9.78 ± 0.908	-0.46 ± 0.027	1.27 ± 0.048
SLH_37548	0.58 ± 0.019	0.24 ± 0.007	-12.86 ± 1.286	-12.72 ± 2.079	-12.35 ± 2.15	-10.88 ± 2.482	-2.75 ± 0.063	9.97 ± 0.048
SLH_39557	0.45 ± 0.006	0.24 ± 0.006	-13.52 ± 0.811	-12.70 ± 0.338	-10.44 ± 0.556	-10.00 ± 0.637	-0.63 ± 0.035	0.12 ± 0.021
SLH_39573	0.45 ± 0.005	0.25 ± 0.006	-13.48 ± 0.633	-12.44 ± 1.207	-10.50 ± 0.688	-9.75 ± 1.127	-0.54 ± 0.035	0.56 ± 0.13
SLH_42795	0.45 ± 0.004	0.23 ± 0.007	-13.52 ± 0.541	-12.73 ± 1.116	-10.57 ± 0.299	-10.01 ± 1.147	0.88 ± 0.038	-0.03 ± 0.089

### 3.2 Equivalent Number of Looks (ENL)

The ENL analysis is typically performed over natural distributed homogeneous targets. In this analysis the test areas used for the analysis were in the Amazonas Rainforest, Antarctica or Greenland Glacier and Sahara Desert. All test data sets were SLC products, meaning that the number of looks is one. Therefore, the measured ENL values should be close to one. The analysis was performed using the SQT software, by manually selecting few homogeneous sub-areas over the scene and calculating the ENL over them. Figure 8 presents an example of the calculated ENL over Greenland, for X4 SM scene 38561.

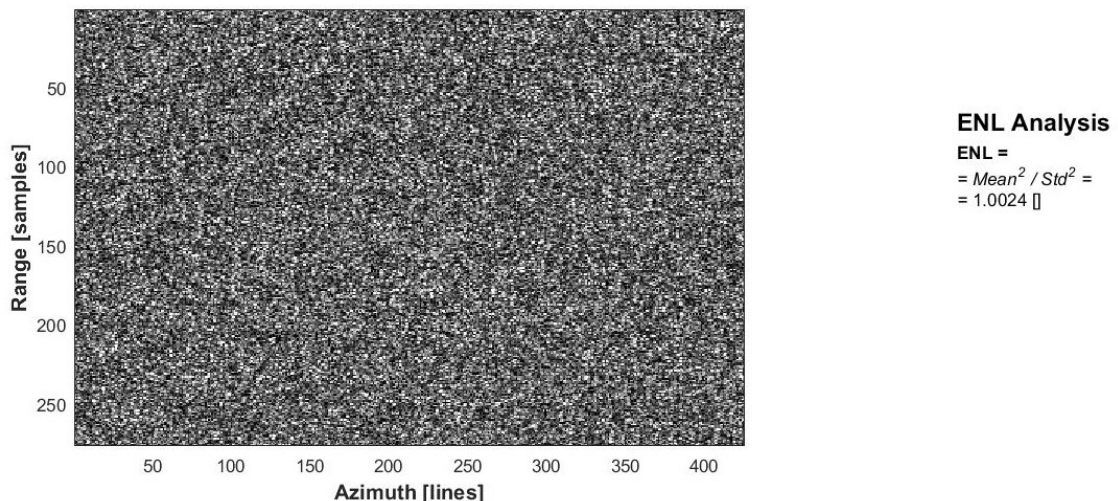


Figure 8: A homogeneous area selected from the SM scene 38561 of X4 from Greenland.

The calculated ENL in the X4 data is shown for the Rainforests in Table 10, Greenland Glacier in Table 11, and Sahara Desert in Table 12. The tables show the average and the std of ENL values calculated from 5 sub-windows selected from each image.

**Table 10. ENL results for X4, Amazon Rainforest.**

Amazon	Average	Std
SL_38159	0.71	0.037
SL_38160	0.73	0.033
SL_38641	0.78	0.040
SL_38642	0.75	0.023
SM_10014	0.83	0.036
SM_38638	0.95	0.007
SM_38639	0.74	0.024
SM_38640	0.74	0.044

**Table 11. ENL results for X4, Greenland Glacier.**

Image ID	Average	Std
SL_38563	1.00	0.005
SL_38564	0.99	0.007
SM_38561	1.00	0.002
SM_38674	1.00	0.001

**Table 12. ENL results for X4, Sahara Desert.**

Desert	Average	Std
SL_38552	1.00	0.017
SL_38631	0.97	0.012
SM_38554	0.98	0.006
SM_38555	0.98	0.024

The calculated ENL in the X6 data is shown for the Rainforests in Table 13, Antarctica Glacier in Table 14, and Sahara Desert in Table 15. The tables show the average and the standard deviation of ENL values calculated from 5 sub-windows selected from each image.

**Table 13. ENL results for X6, Amazon Rainforest.**

Image ID	Average	Std.Dev
SLH_130571	0.80	0.039
SLH_130572	0.78	0.061
SLH_132663	0.77	0.017
SLH_132664	0.74	0.032
SM_130568	0.77	0.025
SM_130569	0.79	0.042
SM_130579	0.78	0.010
SM_132661	0.75	0.043

**Table 14. ENL results for X6, Antarctica Glacier.**

Image ID	Average	Std.Dev
SLH_129954	1.00	0.005
SLH_129955	1.00	0.005
SM_129956	0.99	0.001
SM_132489	1.00	0.002

**Table 15. ENL results for X6, Sahara Desert.**

Image ID	Average	Std
SLH_137302	1.00	0.006
SLH_137313	1.00	0.004
SM_137310	0.98	0.007
SM_137316	0.97	0.019

The calculated ENL in the X7 data is shown for the Rainforests in Table 16, Antarctica Glacier in Table 17, and Sahara Desert in Table 18. The tables show the average and the standard deviation of ENL values calculated from 5 sub-windows selected from each image.

**Table 16. ENL results for X7, Amazon Rainforest.**

Image ID	Average	Std.Dev
SLH_58350	0.65	0.029
SLH_58351	0.64	0.038
SLH_58353	0.44	0.016
SLH_58354	0.44	0.014
SM_58352	0.66	0.012
SM_58356	0.73	0.007
SM_58813	0.65	0.020
SM_58946	0.80	0.006

**Table 17. ENL results for X7, Antarctica Glacier.**

Image ID	Average	Std.Dev
SLH_58812	0.99	0.006
SLH_58838	0.98	0.007
SM_59211	1.00	0.001
SM_59292	0.99	0.006

**Table 18. ENL results for X7, Sahara Desert.**

Image ID	Average	Std
SLH_58369	1.01	0.006
SLH_58864	1.00	0.002
SM_58370	0.97	0.034
SM_58371	0.96	0.028

The calculated ENL for all analysed ICEYE data over the rainforests was clearly under 1, meaning lower than the ideal value of ENL=1 for SLC data. For X4, the ENL was usually close to 0.75, for

X6 between 0.74 and 0.80, and for X7 between 0.44 and 0.73. The calculated ENL for all analysed ICEYE data from the glaciers and the desert was close to the ideal value of ENL=1. The maximum deviation from the ideal value of 1 was only up to 0.2 for the glaciers, and up to 0.4 for the desert sites. Based on the ENL analysis over the glaciers and the desert, the results show correct radiometric signatures of the ICEYE data. The calculated lower ENL in rainforests might be related to the target properties, which might not be homogeneous enough with respect to the fine spatial resolution of the SM, SL and SLH data.

### 3.3 Noise Equivalent Sigma Zero (NESZ)

One of the most essential quality indicators in SAR is the noise equivalent sigma zero (NESZ), showing the contribution of noise in the observed backscatter. Weaker NESZ is an indication of higher quality SAR data, because targets with relatively low backscatter can be identified with less noise disturbance. Table 19 shows the NESZ values for each satellite and imaging mode provided in the ICEYE documentation.

**Table 19: The NESZ values (dB) provided in the ICEYE documentation, for each analysed ICEYE satellite and imaging mode.**

	X4	X6	X7
SM	-19	-20	-20
SL	-17		
SLH	-15	-15	-15

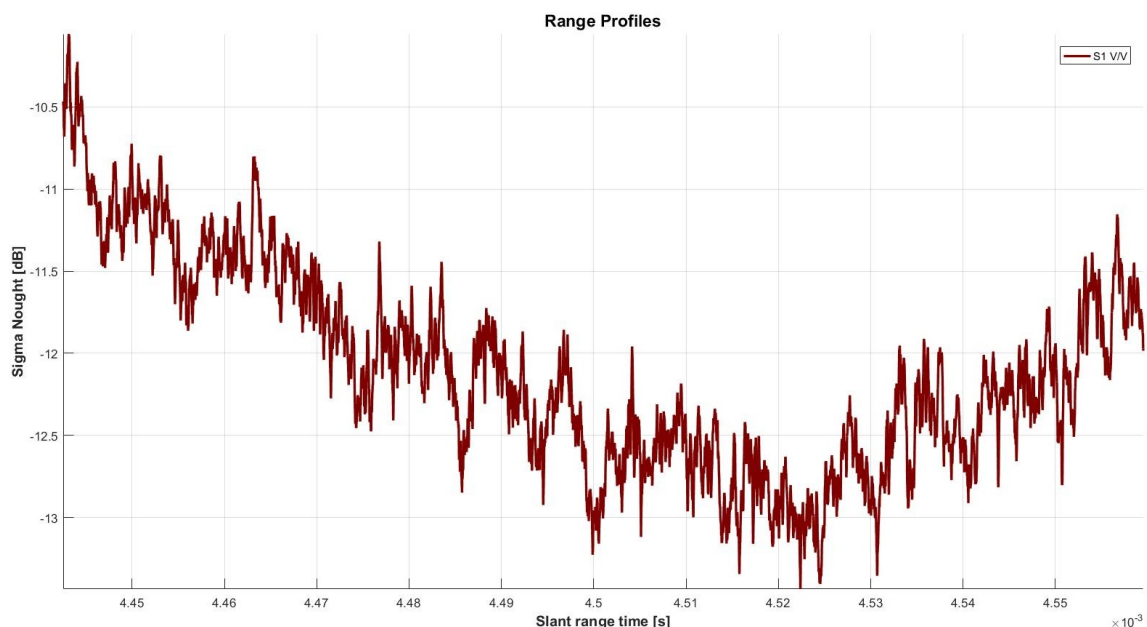


**Figure 9: Range profile example from the SM scene 33037 of X4 acquired from the Atlantic Doldrums, used for the NESZ calculation.**

The NESZ is assessed using the SQT by manually extracting and plotting a range profile of the sigma nought ( $\sigma^0$ ) backscatter from low backscatter targets. Few sub-areas within the images with the lowest possible backscatter are selected to perform the analysis. Since there may be some residual backscatter even in the selected areas, the minimum of the range profile graph showing the lowest backscatter can be considered the NESZ value, assuming that the contribution of the

target itself to the observed backscatter power is negligible. Figure 9 shows an example of a range profile extracted from the SM image 33037 of X4 over the Atlantic Doldrums.

Table 20, Table 21 and Table 22 list the measured NESZ values for the X4, X6 and X7 data, respectively. The values in the tables are the lowest calculated average values of the radiometric profiles. For all analysed satellites, the NESZ was measured over three low backscatter test sites: Atlantic Doldrums, Pacific Doldrums, and the Sahara Desert. Data with the shallowest (highest) possible incidence angle was chosen for the NESZ analysis.

**Table 20. NESZ for the X4 scenes of the Atlantic Doldrums, Pacific Doldrums and Sahara Desert.**

Atlantic Doldrums		Pacific Doldrums		Sahara Desert	
Image ID	NESZ (dB)	Image ID	NESZ (dB)	Image ID	NESZ (dB)
SL_33032	-11,1	SL_33040	-11.4	SL_38552	-12.2
SL_33033	-12,5	SL_33041	-11.6	SL_38631	-13.1
SM_33037	-13,5	SM_33044	-13	SM_38554	-16.6
SM_33039	-16,7	SM_33045	-14	SM_38555	-25.9

**Table 21: NESZ for the X6 scenes of the Atlantic Doldrums, Pacific Doldrums and Sahara Desert.**

Atlantic Doldrums		Pacific Doldrums		Sahara Desert	
Image ID	NESZ (dB)	Image ID	NESZ (dB)	Image ID	NESZ (dB)
SLH_129810	-9.3	SLH_129811	-12.5	SLH_137302	-9.5
SLH_129813	-10.2	SLH_129812	-13.0	SLH_137313	-9.3
SM_129957	-10.6	SM_132461	-13.7	SM_137310	-12.3
SM_129959	-10.1	SM_132475	-11.0	SM_137316	-12.7

**Table 22: NESZ for the X7 scenes of the Atlantic Doldrums, Pacific Doldrums and Sahara Desert.**

Atlantic Doldrums		Pacific Doldrums		Desert	
Image ID	NESZ (dB)	Image ID	NESZ (dB)	Image ID	NESZ (dB)
SLH_67166	-13,3	SLH_98795	-13,5	SLH_58369	-12,3
SLH_67901	-12,9	SLH_103086	-13,2	SLH_58864	-12,4
SM_58358	-14	SM_58359	-17,2	SM_58370	-15,9
SM_58360	-20,3	SM_58363	-20,8	SM_58371	-16,1

The measured NESZ values are mostly higher than the values provided by ICEYE. For X4 only one, for X6 none, and for X7 two of the analysed scenes have NESZ in line or better than the values in the ICEYE documentation. The measured strong NESZ could however be caused by an overestimation due to the method used in the SQT. When calculating the  $\sigma^0$  range profiles, all pixels in the azimuth direction are averaged, rather than choosing only the low backscatter pixels in the averaging. Another possible reason for the relatively high observed NESZ is the difficulty in finding areas with very low backscatter, as the shallowest possible incidence angle offered by ICEYE is only 30-35 degrees.

### 3.4 Elevation Antenna Pattern

The observed backscatter needs to be corrected for changes caused by the antenna elevation angle in the range direction. A pre-defined antenna elevation pattern (AEP) is used by the data

provider for compensating the contribution of the elevation angle to the measured gain. In this section we assessed whether the AEP correction was applied correctly on the data. The images were analysed by averaging the backscatter in azimuth direction and extracting range profiles of the averaged backscatter in slant range time units. The backscatter was then normalized by the inverse of the average measured backscatter. The analysis was performed on the Rainforest scenes, where the noise component can be considered negligible (very low) compared to the target backscatter level. Gamma nought ( $\gamma^0$ ) backscatter was chosen because it is independent of the incidence angle with the ground surface. Ideally, the normalized  $\gamma^0$  range profiles should be horizontal, with a value of zero dB all along the x-axis.

The figures below (Figure 11 - Figure 16) show the normalized antenna pattern with respect to the slant range time, extracted from the analysed SAR images. Figure 11 shows the AEP of the SLH scenes and Figure 12 the AEP of the SM scenes of the X4 satellite. Similarly, Figure 13 and Figure 14 show the AEP of the SLH and the SM scenes of X6, and Figure 15 and Figure 16 the SLH and SM AEP profiles of X7.

Generally, the AEP correction performed by the data provider was more successful for the SLH and SL imaging modes than for the SM mode. This is expected, as the antenna elevation varies more in the wider SM images, thus making it harder to compensate for the effect of the elevation angle. The best AEP correction has been applied to X4 SL scenes, as seen from the horizontal profiles with a 0.5 dB maximum deviation of the trend line from zero level for the scenes 38159 (upper left), 38160 (upper right) and 38642, and a 1 dB maximum deviation for the scene 38641 (lower left). The AEP correction for the SLH scenes of X6 and X7 was good, apart from the relative low backscatter in the near range (seen as higher normalized  $\gamma^0$  values in the left end of the profiles). Figure 10 shows a sub-area of a X6 SLH scene, where the relatively low backscatter in the near range can be seen in the left side of the image. Apart from the very near range in X6 and X7, the AEP correction can be therefore considered successful for the SL and SLH data.

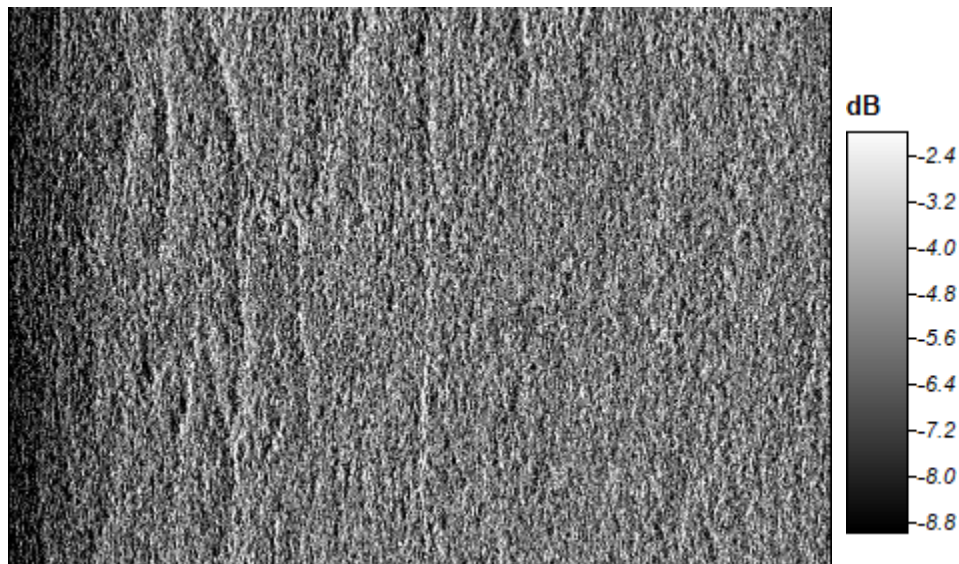


**Figure 10: A sub-area extracted from the X6 SLH scene 130571, covering the whole scene in the range direction. The relatively low backscatter level in the near range end can be seen clearly in the left side of the image.**

Concerning the SM imaging mode, where the AEP correction is more challenging, the correction of the antenna elevation was less successful. As seen in the profiles of the SM scenes (Figure 12 for X4, Figure 14 for X6 and Figure 16 for X7), the  $\gamma^0$  backscatter along the range direction is not horizontal. For some SM scenes there is a linear increasing or decreasing trend with backscatter change of 1-3 dB from near to far range, and for some of the scenes the  $\gamma^0$  profiles have a parabolic shape. In most of the SM scenes there is a combination of linear and parabolic behaviour in the AEP profiles. The parabolic shape can be related to increased noise in the images, but the linear behaviour is most likely related of the changing antenna elevation angle.

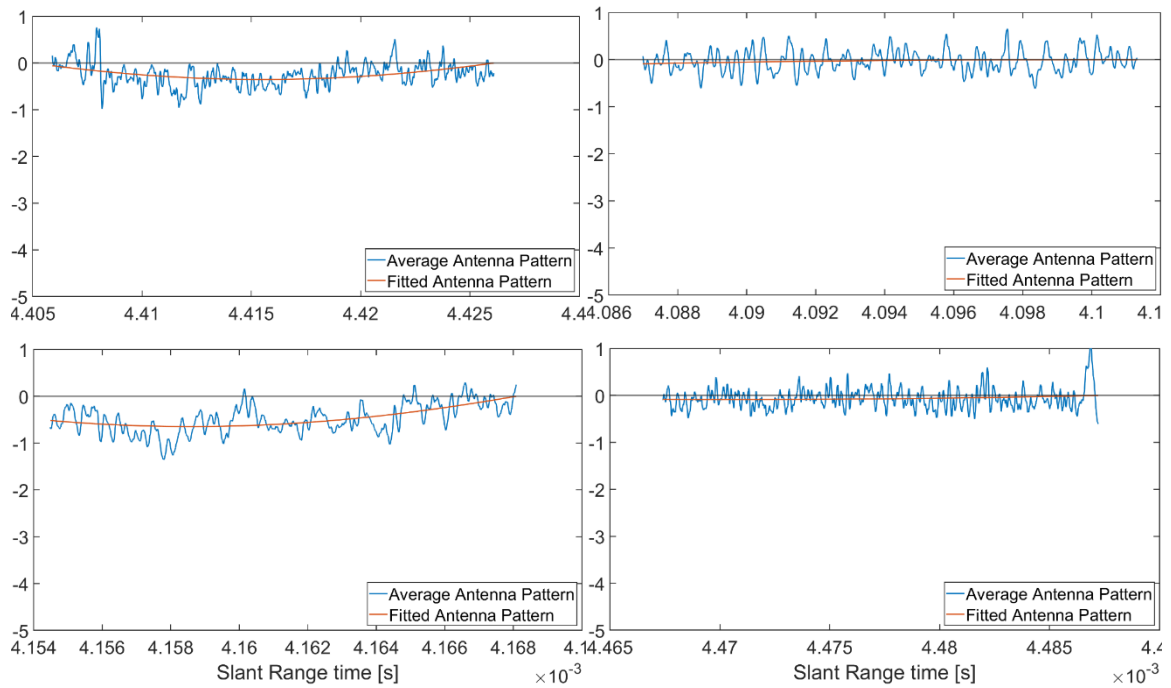


Figure 11. EAP for the X4 SL images 38159 (upper left), 38160 (upper right), 38641 (lower left) and 38642 (lower right).

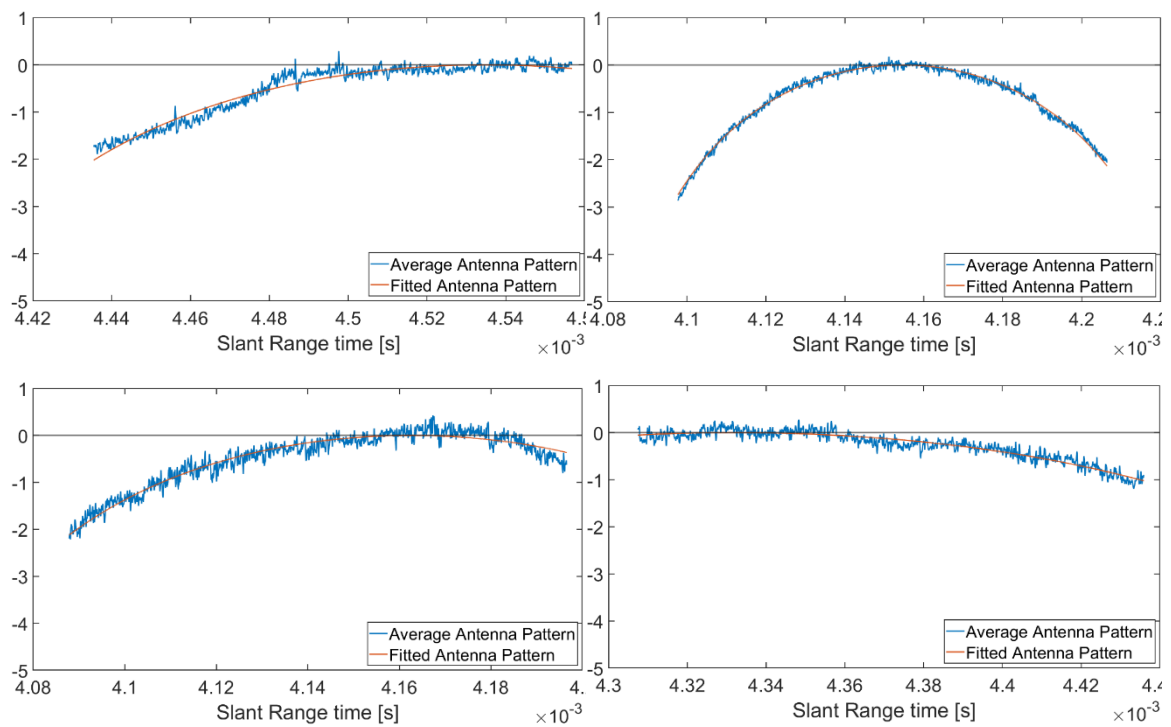


Figure 12. EAP for the X4 SM images 10014 (upper left), 38638 (upper right), 38639 (lower left) and 38640 (lower right).

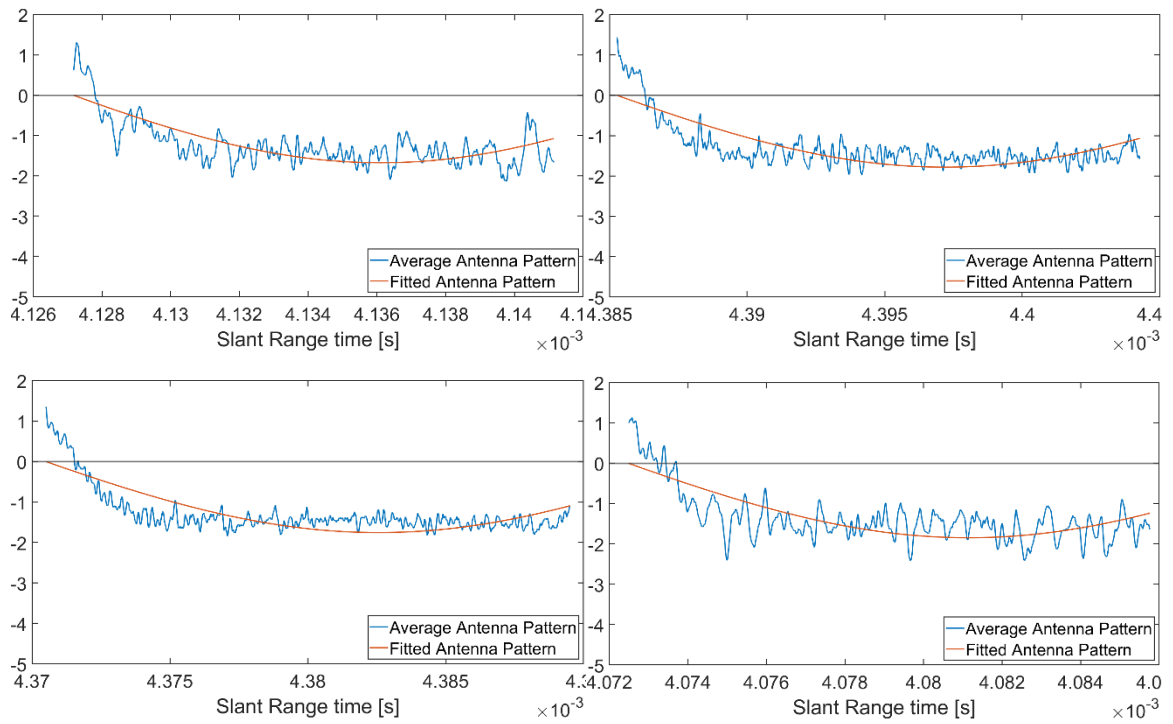


Figure 13: EAP for the X6 SLH images 130572 (upper left), 130571 (upper right), 132663 (lower left) and 132664 (lower right).

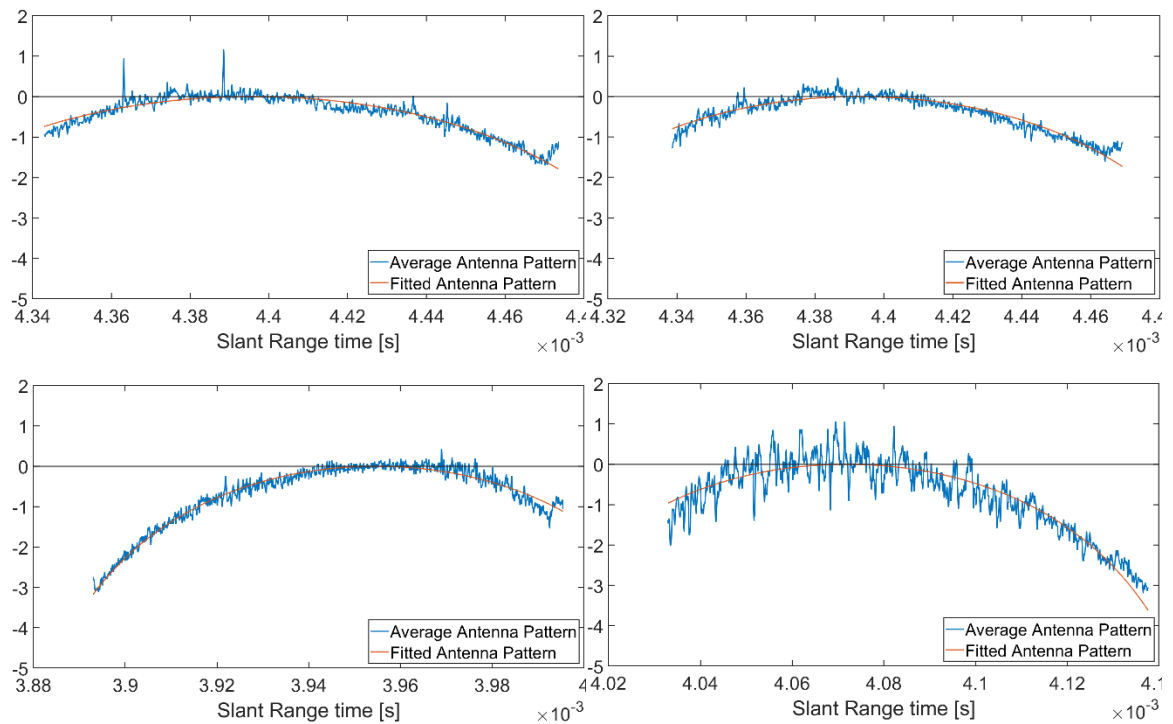
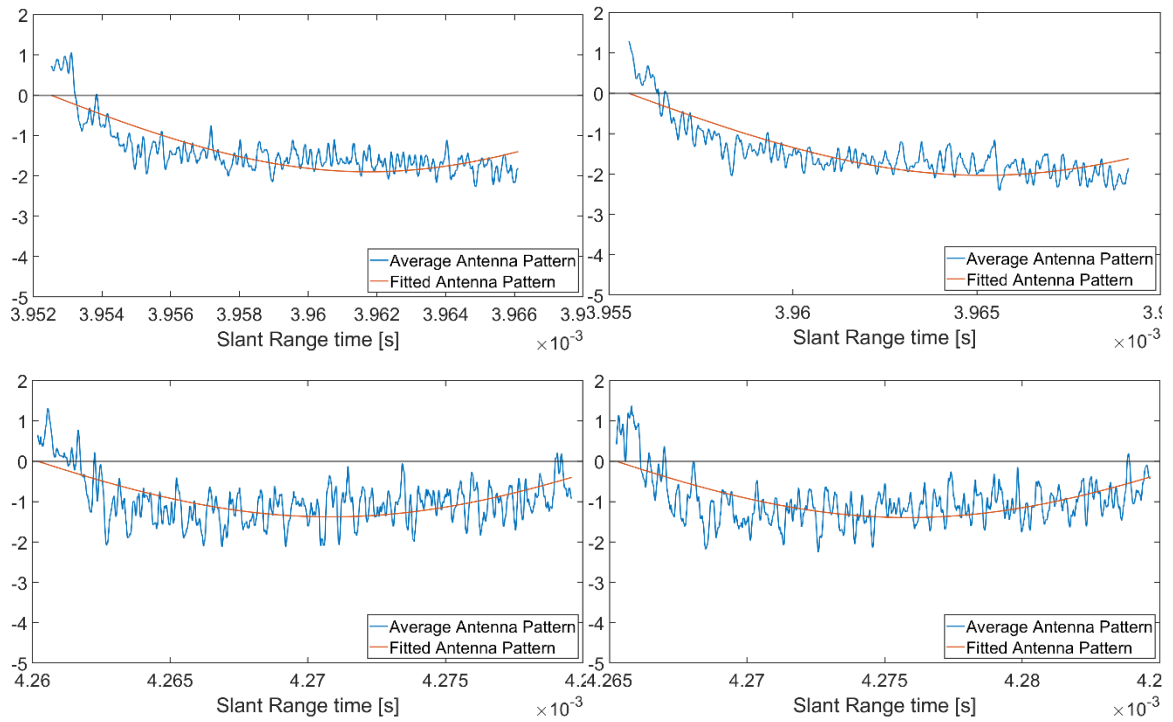
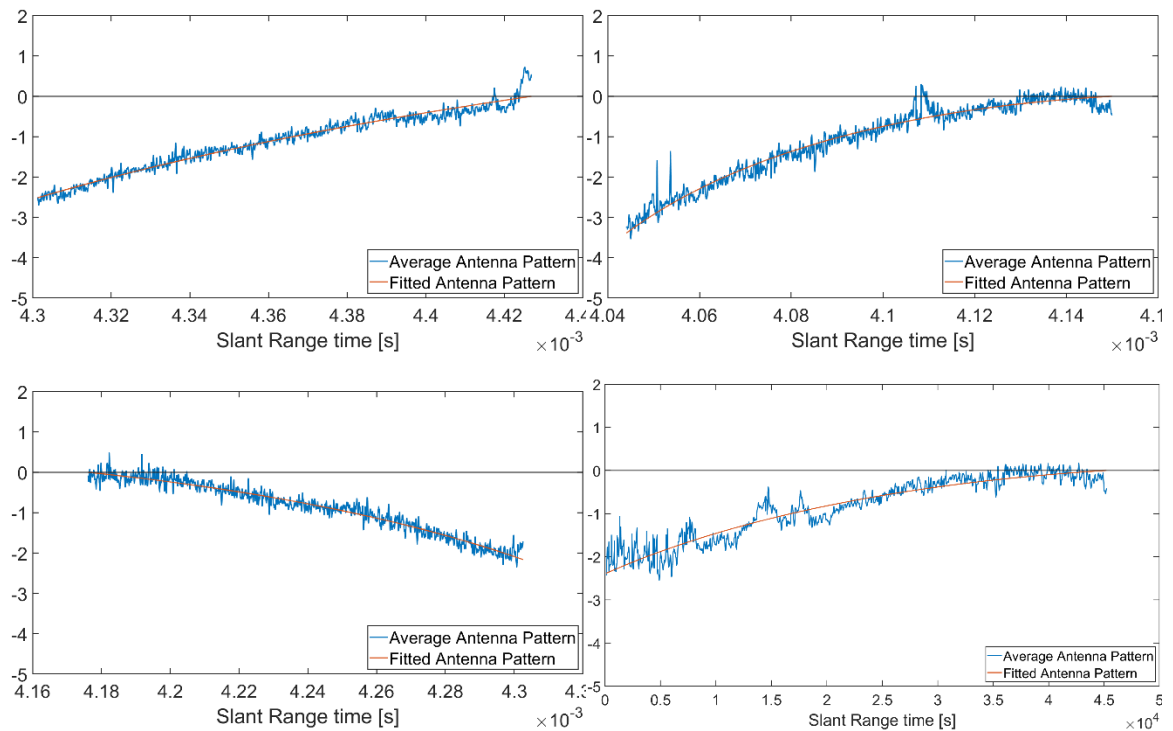


Figure 14: EAP for the X6 SM images 130568 (upper left), 130569 (upper right), 130579 (lower left) and 132661 (lower right).



**Figure 15: EAP for the X7 SLH images 58350 (upper left), 58351 (upper right), 58353 (lower left) and 58354 (lower right).**



**Figure 16: EAP for the X7 SM images 58352 (upper left), 58356 (upper right), 58813 (lower left) and 58946 (lower right).**

### 3.5 Radiometric Stability

The radiometric stability and consistency reflect the ability of the satellite measurements to repeatedly produce similar calibrated backscatter values from targets having the same properties. Better radiometric stability thus enables the users to correctly analyse and interpret multiple observations acquired at different times or from different locations having the same target properties. The radiometric stability of SAR is usually tested over rainforests, because they present a spatially homogeneous backscatter with small seasonal changes and low dependency on incidence angle. The absolute radiometric accuracy (within one data scene and over time) derived during the commissioning phases by ICEYE was 2 dB RMSE (RD-3). The relative radiometric accuracy, indicating the std of the observations within one data scene is 1 dB, a value provided in the ICEYE web site.

For assessing the radiometric stability all acquired data from the Amazonas Rainforest are analysed. A representative sub-area covering the whole range axis was first chosen from each image. The selected areas were then calibrated to  $\sigma^0$  backscatter. Finally, the average and the std of the observed backscatter were calculated from the linear power units. The average and the std for each analysed scene are presented in Table 23. The average values are shown in decibel units, but the std is given in linear power units. The colours of the cells indicate the level of consistency in relation to the most typical observed value of approximately -5 dB. The green colour indicates good radiometric stability, with a deviation less than 0.5 dB from the most typical value. The light green, yellow and orange colours refer to moderate, poor, and very poor radiometric stability, with deviations of 0.5-1.5 dB, 1.5-2.5 dB, and over 2.5 dB from the most typical backscatter value of -5 dB, respectively.

Generally, the radiometric stability of the ICEYE data can be considered reasonable, with a backscatter variation usually less than 1 dB from the most typical -5 dB level. The stability is somewhat better for the SLH and SL data compared to the SM data, maybe due to the smaller variation in the antenna elevation range (see section 3.4). An improvement in the radiometric stability towards newer satellites and/or processor versions can be seen, especially for the SM data (see processor versions in Table 1, Table 2 and Table 3).

**Table 23: Radiometric stability of the ICEYE satellites over the Amazonas Rainforest. The average in dB units and the std in linear units for each scene is listed. Green, light green, yellow and orange cell colours indicate a deviation of up to 0.5 dB, 1.5 dB, 2.5 dB, or more than 2.5 dB from the typical backscatter value of -5 dB, respectively.**

Imaging mode	X4	X6	X7
SM	-1.96 ± 0.80	-5.07 ± 0.36	-4.14 ± 0.48
	-7.76 ± 0.18	-5.73 ± 0.31	-6.55 ± 0.28
	-8.61 ± 0.16	-7.48 ± 0.22	-5.15 ± 0.39
	-5.61 ± 0.33	-6.65 ± 0.27	-5.43 ± 0.36
SL	-6.73 ± 0.27		
	-4.59 ± 0.44		
	-4.93 ± 0.41		
	-5.44 ± 0.38		
SLH		-5.63 ± 0.32	-4.26 ± 0.50
		-5.93 ± 0.32	-4.58 ± 0.46
		-5.49 ± 0.33	-4.76 ± 0.51
		-6.13 ± 0.31	-4.77 ± 0.51

### 3.6 Data Processing in SNAP – Geolocation Accuracy

The geolocation accuracy and the processing of the ICEYE data using the publicly available SNAP software were evaluated for the X4 and X6 data acquired from the Helsinki airport, Finland. X7 data was not acquired from this test area, as we preferred having relatively more scenes from Kiruna site that contained only one relevant CR for the IRF analysis. There were no CRs installed in the Helsinki airport area, so IRF analysis was not performed. Instead, georeferenced and calibrated images were produced in SNAP, and the SAR images were compared against known reference targets on the ground.

The data were processed in SNAP version 8.0. No external plugin was needed for processing the data, as from version 8.0 onwards the software contains a processor for the ICEYE data as a default. The processing steps included image subsetting, calibration to  $\sigma^0$  backscatter, terrain correction and speckle filtering. The images were geocoded to the ETRS89-TM35FIN coordinate reference system and saved in GeoTIFF file format. A DEM of 10 m cell size acquired from the National Land Survey of Finland (NLS) was used in the terrain correction. The processing of the ICEYE data in SNAP was successful. Figure 17 shows a processed X4 SL image with polygons depicted using the airport runways and a service road in the airport area.

The distances between the known location of the targets and the location of the targets on the SAR images were measured manually in a GIS software. The airport runways were used as the reference targets for the geolocation accuracy assessment. Their locations were derived from a 1:5000 scale (0.5 m resolution) map generated by NLS of Finland.

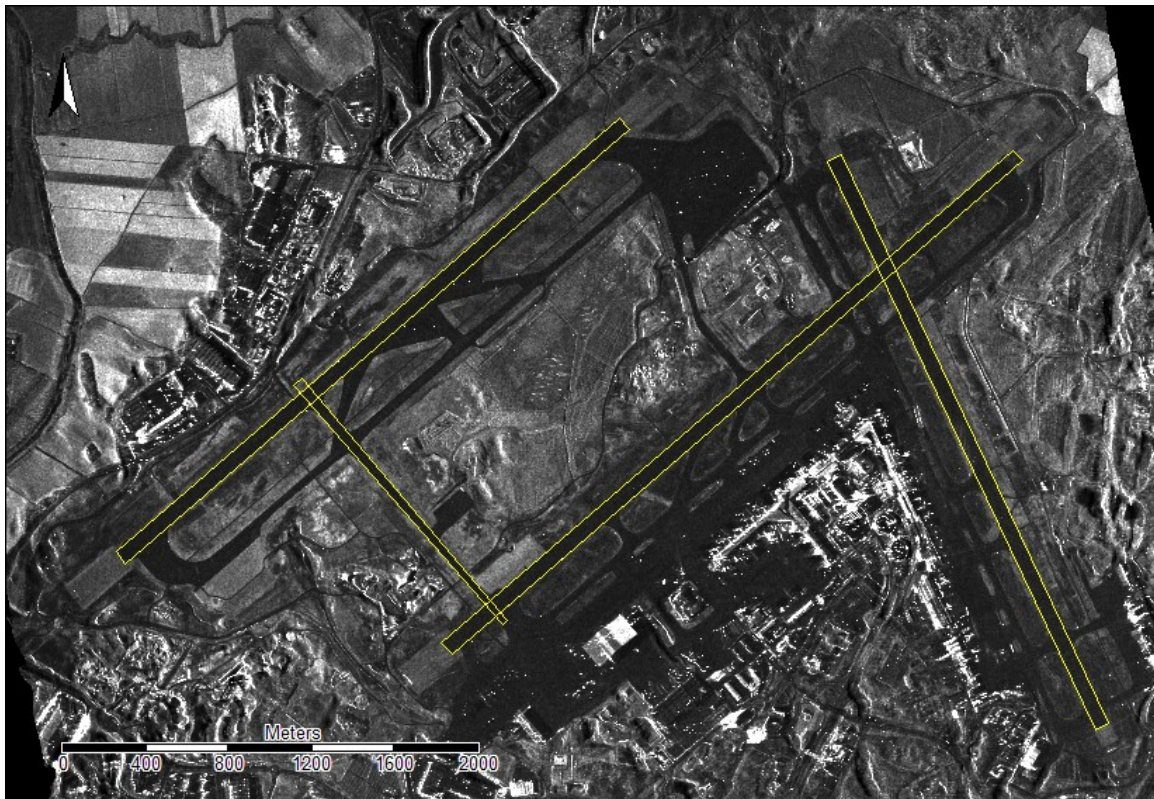


**Figure 17: The Helsinki airport area as seen in a X4 SL image. The runways and one service road are manually depicted over the SAR image, and their location is compared against the spatial data of the NLS.**

The measured geolocation errors in x-axis (East-West) and y-axis (South-North) directions, the total error in 2D space (Euclidian distance), and the mean and std of the measured geolocation errors are listed in Table 24 for X4 and Table 25 for X6 data. The measured geolocation mean error (ME) was typically around 20 m, which is notably larger than the values measured in the IRF

analyses, and the localization uncertainty values provided by ICEYE (9 m). There were few scenes with even more significant localization errors between 30 and 100 m. It should be noted that the more robust and meaningful geolocation accuracy assessment is done in Section 0 using the CR test sites of Rosamond, Sodankylä and Kiruna. The localization accuracy assessed in this section is prone to errors in the manual measurements (while depicting the targets), the used DEM, the reference spatial dataset, and the ICEYE data processor in the SNAP software.

**Table 24: Observed geolocation error in the X4 scenes over Helsinki Airport. dx and dy refer to the error in x-axis (East-West) and y-axis (South-North). dl refers to the total Euclidian distance in 2D space. The mean error (ME) and the std are calculated from the measurements of both runways.**

	SM_20201017			SM_20201019			SL_20201016			SL_20201111			SLH_20201016			SLH_20201107		
	dx	dy	dl	dx	dy	dl	dx	dy	dl	dx	dy	dl	dx	dy	dl	dx	dy	dl
RW1	-8	21	22	-59	-79	99	-8	20	22	-3	22	22	24	-4	24	43	26	50
RW2	-10	18	21	-60	-84	103	-10	17	20	-1	17	17	25	-3	25	44	23	50
ME	-9	19,5	21,5	-59,5	-81,5	101	-9	18,5	21	-2	19,5	19,5	24,5	-3,5	24,5	43,5	24,5	50
std	1	1,5	0,5	0,5	2,5	2	1	1,5	1	1	2,5	2,5	0,5	0,5	0,5	0,5	1,5	0

**Table 25: Observed geolocation error in the X6 scenes over Helsinki Airport. dx and dy refer to the error in x-axis (East-West) and y-axis (South-North). dl refers to the total Euclidian distance in 2D space. The mean error (ME) and the std are calculated from the measurements of both runways.**

	SM_137630			SM_137631			SLH_137632			SLH_137633		
	dx	dy	dl	dx	dy	dl	dx	dy	dl	dx	dy	dl
RW1	-3	20	20	14	26	30	-3	16	16	-3	16	16
RW2	-2	18	18	16	28	32	0	17	17	0	17	17
ME	-2,5	19	19	15	27	31	-1,5	16,5	16,5	-1,5	16,5	16,5
STD	0,5	1	1	1	1	1	1,5	0,5	0,5	1,5	0,5	0,5

## 4. CONCLUSIONS

An assessment of the available ICEYE documentation and the ICEYE X4, X6 and X7 test data was performed by FMI. The documentation was found to be overall in a good level. The openly available “SAR Product Guide” (RD-1) and “Level 1 Product Format Specification Document” (RD-2) provided the necessary basic information regarding the data products and properties. Some of the required information for our assessment of the earlier X4 data was found in the previous versions of the Product Guide (RD-3) and Product Format Specification (RD-4) documents. The radiometric calibration and validation of the X2-X5 satellites performed by ICEYE are described in the “Data Calibration and Validation, version 1.0” document (RD-5). Documents which are not publicly available, describing the more detailed quality analyses performed internally by ICEYE, were also provided to the EDAP assessment team (RD-6 – RD-8). These documents provided a good theoretical background and presented the methods used and the obtained results in a clear manner. Documents describing the calibration and validation of the X6 satellite were not yet available at the time of writing this document.

An independent data analysis of the test datasets was performed by FMI using mainly the SQT software of Aresys. In this work we evaluated the Stripmap (SM), Spotlight (SL) and Spotlight High resolution (SLH) imaging modes. The relevant parameters describing the SAR data quality were calculated and compared with the corresponding values provided by ICEYE in the available documentation. The measured IRF quality metrics were generally found to be in line with the values provided by ICEYE. The spatial resolution was mostly in line or even better than the values provided by ICEYE. The ISLR was typically within the expected range, while the PSLR was sometimes higher (worse) than the provided values. If compared with corresponding SAR data of other data providers, the ICEYE products have a higher spatial resolution, but relatively strong side lobes, because no windowing function such as Taylor, Hanning, Hamming or Kaiser is applied during data processing. The measured localization errors were typically in line with the CEP90 localization error provided by ICEYE.

The measured NESZ was usually higher than the values provided by ICEYE. The strong NESZ could however be caused by the relatively basic calculation method applied by the SQT software, or due to the difficulty in finding areas with very low backscatter for the relatively steep incidence angle ICEYE data. The measured ENL in the Glacier and the Desert sites was very close to the ideal value of ENL=1, reflecting a correct radiometric distribution of the ICEYE data. The ENL in rainforests was typically less than the expected value of ENL=1, probably due to the difficulty in finding entirely homogeneous regions in the rainforests for the relatively high-resolution data. The AEP correction performed by ICEYE was reasonable for the SL and SLH products, although for X6 and X7 data the backscatter was relatively low in the near range end. For the SM data having a larger variation of the antenna angle, the AEP correction was less successful. Linear decreasing or increasing trends in the gamma nought backscatter ( $\gamma^0$ ) profiles were found in many of the analysed scenes. The shape of the  $\gamma^0$  profile was sometimes parabolic, which could be related to an increased radiometric noise level in the image. The radiometric stability was usually in line with the radiometric accuracy of 2 dB RMSE measured by ICEYE in the commissioning phases. The backscatter deviation from the most typically observed level was mostly less than 1 dB. The higher resolution SL and SLH imaging modes were generally more radiometrically consistent than the SM data, especially for the X4 satellite. The radiometric stability improved towards newer satellites and/or processor versions.

The ICEYE data was successfully processed in the publicly available SNAP software, including basic SAR operations such as calibration, geometric correction, and speckle filtering. The localization errors measured against known locations in Helsinki were larger than expected, but these are also influenced by the accuracy of the manual measurements, the used DEM, the reference data, and the ICEYE data processor in SNAP.

Based on the assessment presented in this document, the ICEYE SAR data can be generally considered of good quality relative to the uncertainty values stated by the data provider. Documents describing the data products and the calibration and validation activities performed internally by ICEYE were comprehensive and covered all relevant information.

## 5. REFERENCES

- RD-1 SAR Product Guide version 4.1, released in 1/5/2021. Available online: <https://www.iceye.com/sar-data/documents> (11/2021)
- RD-2 SAR Product Guide, version 3.0, released in 1/5/2020.
- RD-3 Level 1 Product Format Speciation Document, version 2.1, released in 11/6/2020. Available online: <https://www.iceye.com/sar-data/documents> (11/2021)
- RD-4 Level 1 Product Format Speciation Document, version 1.0, released in 5/7/2019.
- RD-5 Data Calibration and Validation, version 1.0, released 22/6/2020. Available online: <https://www.iceye.com/sar-data/documents> (11/2021)
- RD-6 ICEYE IRF Quality Parameters Assessment for X2-X5, Not public
- RD-7 ICEYE SAR Data Geolocation for X2-X5, Not public
- RD-8 ICEYE Data Quality Assessment for X7, Not public